Handbook of Advanced Ceramics
S. Sōmiya *et al.* (Eds.)

CHAPTER 3

3.1 Forming and Drying

YUNPENG YANG, ERIC LAARZ, SUNITA KAUSHIK,
ERIK MUELLER and WOLFGANG SIGMUND
Department of Materials Science and Engineering, University of Florida, Gainesville, FL 32611-6400, USA

3.1.1 INTRODUCTION

Ceramic processing is an exciting field that requires the combination of knowledge from several scientific disciplines such as surface chemistry, solution thermodynamics, polymer physics, quantum mechanics, and colloid science. This chapter will introduce the fundamentals of some of these sciences with a specific view for ceramic processing and highlight recent findings. Furthermore, it will give some practical guidance on forming and drying by summarizing the published literature. The intention of this chapter is not to be complete since each of the scientific fields has a vast body of literature. We will refer to review articles and books that will allow for further reading.

Due to the high melting temperatures exceeding most other materials ceramic materials are typically not melt processed as is for metals or polymers. Therefore, 90% of the world markets in ceramics are materials derived from powders. Before sintering, these powders have to be handled and processed. Since most of the desired properties of advanced ceramics have microstructures of micron and sub-micron size ceramic powders with particle sizes in the sub-micron range are applied. As soon as the particle diameter drops below 100 μm surface forces are being about equal as the gravitational pull on the particles, yielding agglomerates for particles that are smaller than 100 μm. For particles sizes of 1 μm to 1 nm, surface forces dominate their behavior in processing being 3–10 orders of magnitude larger than gravitational forces. Therefore, a full understanding of surface forces or colloidal forces is required in order to be able to control ceramic powder processing on an advanced level. The science of colloids especially the origin of surface forces and their quantitative measurement will be presented in the beginning. It should be stressed that even for processes that use dry pressing of granules the particles had been processed in slurry at some point (Fig. 3.1.1).

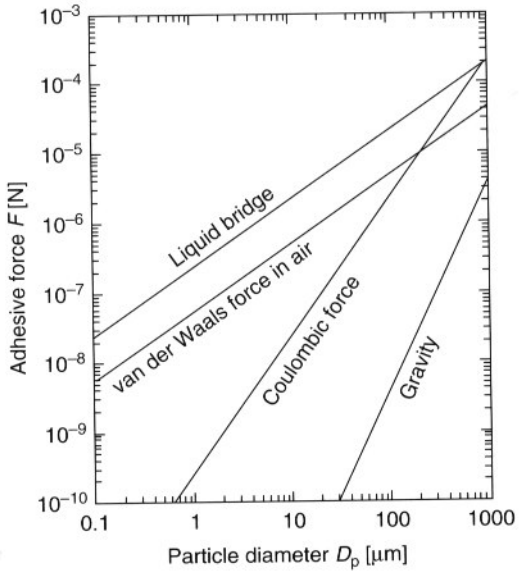

FIGURE 3.1.1 Comparison of adhesive surface forces depending on particle size [1].

After the introduction to colloid science for ceramic processing, ceramic forming techniques will be presented. First the casting techniques can be divided into two categories, that is, drained casting and constant volume casting. Drained casting techniques solidify slurry by removal of the dispersing media that goes along with shrinkage of the consolidating body, examples are slip casting or pressure slip casting. Constant volume techniques solidify the slurry without removal of the dispersing medium.

The next steps in processing are drying and binder burnout. Here, we additionally introduce a section on green body characterization since there has been tremendous progress in this field. Furthermore, sintering has only limited capability of healing flaws caused in processing before firing. Therefore, finding flaws and relating them to causes of the processing steps is most important to eliminate them from the processing cycle.

3.1.2 FUNDAMENTALS OF POWDER PROCESSING

3.1.2.1 General Concepts and Theories in Colloidal Processing

Due to the size range of advanced ceramic powder particles, that is, sub-micron and nowadays, nanometer size it is essential to understand the sciences behind

particulate behavior of these objects. Objects that have at least one dimension in the range of 1 nm to 1 μm are considered colloids. The term comes from the Greek word for "glue" since these materials have the tendency to stick.

In ceramic processing these surface forces that cause sticking have to be controlled. In order to produce slurry with desirable properties, a number of suspension parameters must be carefully considered. Stability is the most desired property in a ceramic suspension. Interparticle forces play an important role in deciding the stability of the slurry. Particles suspended in a liquid medium will spontaneously agglomerate due to the attractive van der Waals forces between the surfaces. To prevent this spontaneous flocculation, modifications to the particle surface have to be made in order to produce a repulsive potential that can counteract the attractive van der Waals potential. High solids' loading is another desirable property in slurry. Generally, it is preferable to have as high a solids content as possible and yet have a low enough viscosity for the slurry to be fluid for filling molds or spray drying.

3.1.2.1.1 Origin of van der Waals Forces

Attractive forces between atoms and molecules were discovered by van der Waals when he had to make changes (add a finite volume and add attractive forces) to the ideal gas law (Boyle's law) in order to make it work for real gases over a broader temperature range. Since then several physicists explained the origin of these attractive forces. Typically three fundamental origins are described, the so-called Keesom forces, the Debye forces and the London or dispersion forces. The first two require at least one permanent dipole and the last depends only on transient dipoles inducing dipoles in neighboring atoms or molecules. Hamaker was the first to describe these energies more quantitatively in 1937. He showed that the energy of van der Waals attraction (E_{vdW}) equals a materials constant (A) times a distance (d) and body geometry dependent function $G(d)$.

$$E_{vdW} = A \times G(d) \tag{1}$$

Nowadays, A is referred to as Hamaker constant. Although this material-specific Hamaker constant is fundamentally important the number of materials where these numbers are known for are very limited. This has to do with the fact that the theoretical and experimental access to Hamaker constants still proves difficult. We refer the interested reader to two excellent review papers on Hamaker constants and van der Waals forces in ceramic processing by L. Bergström and R. French [2, 3].

3.1.2.1.2 Stabilization of Colloidal Suspensions

Dispersing particles by making them mutually repulsive is called "stabilization". It can be achieved by segregating either charged ions or polar molecules in

solution preferentially to the particle surface (electric double layer stabilization), by adsorbing polymer chains onto the particles (steric stabilization) or by a combination of the two mechanisms (electrosteric stabilization).

3.1.2.1.2.1 *Electric double layer forces*

The surface charge of a colloidal particle in a suspension forms the basis of electric double layer stabilization. The magnitude of surface charge determines the magnitude of repulsion between the particles and thus the stability of the slurry. Oppositely charged ions (counterions) and oppositely charged ends of polar molecules in solution get attracted to this charge on the surface of the particle, resulting in the formation of a "diffuse double layer" of ions. Guoy and Chapman developed this theoretical concept of the double layer in the early twentieth century. For a particle surrounded by the diffuse double layer the shear slippage will occur at some distance from its surface. The electric potential at this shear slippage plane is called the zeta potential. The zeta potential is the potential at the surface of the electrokinetic unit moving through the liquid medium [4].

The main mechanism by which oxide particles develop a surface charge is by adsorption of ions from solution. The surfaces of the oxide particles are normally hydrated in water. Adsorption of H^+ ions produces a positively charged oxide surface at low pH, whereas at high pH the adsorption of OH^- ions produces a negatively charged oxide surface. The pH at which the surface is neither negatively nor positively charged is known as the point of zero charge (Fig. 3.1.2).

The inner and the outer Helmholtz layer together form the Stern layer. The value of the zeta potential is believed to be close to the potential at the Stern layer. Hence, it is more practical to measure the zeta potential. The pH value at which the zeta potential is zero is called the iso-electric point (IEP). The IEPs of various compounds are given in Table 3.1.1.

Theoretically, the relationship between surface charge density σ_0 and surface potential ϕ_0 of a particle dispersed in a liquid is given by [4]

$$\sigma_0 = (8\varepsilon\varepsilon_0 RTc)^{1/2} \sinh\left(\frac{zF\phi_0}{2RT}\right) \tag{2}$$

where ε is the dielectric constant of the medium, ε_0 the permittivity of free space, R the gas constant, F the Faraday constant, c the concentration of the electrolyte ions and z the valence of the electrolyte ions. For low potentials (i.e. when ϕ_0 is less than ~50 mV), the above equation becomes

$$\sigma_0 = \varepsilon\varepsilon_0\kappa\phi_0 \tag{3}$$

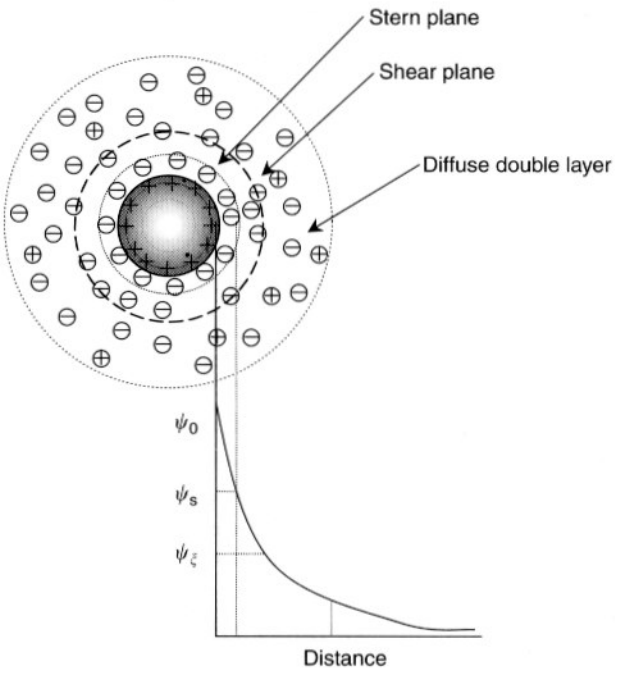

FIGURE 3.1.2 Electric double layer. The electric potential as a function of distance from the particle surface. The distance equal to $1/\kappa$ is the Debye length. ψ_s = surface potential; ψ_ζ = zeta potential; ψ_0 = zero potential.

TABLE 3.1.1 Nominal Iso-Electric Points of Oxides

Material	Iso-electric point
α-Alumina (Al_2O_3)	9–9.5
Silica (SiO_2)	3–4
Zinc oxide (ZnO)	9
Titania (TiO_2)	4–5
Calcium carbonate ($CaCO_3$)	9–10
Lead oxide (PbO)	10
Magnesia (MgO)	12–13
Zirconia (ZrO_2)	4–5
Stannic oxide (SnO_2)	4–7

where $1/\kappa$ is referred to as the thickness of the double layer or the Debye length and is defined by

$$\kappa^2 = \frac{2cz^2F^2}{\varepsilon\varepsilon_0 RT} \tag{4}$$

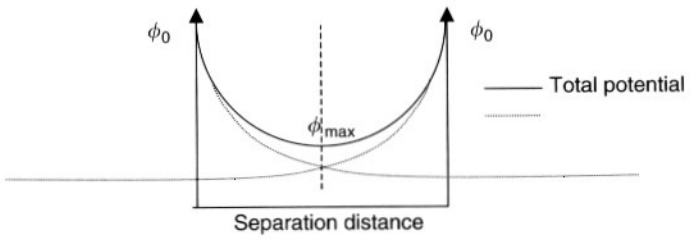

FIGURE 3.1.3 Overlap of electric double layers due to approach of two parallel surfaces, resulting in an increase in the ionic concentration, which results in repulsion between them.

3.1.2.1.2.2 *Repulsion between double layers*

Considerable importance has to be given to the double layers around colloidal particles when they approach each other. When two particles with like charges approach each other, their double layers start overlapping as soon as there is considerable interpenetration of the two diffuse layers (Fig. 3.1.3).

The overlap of the ionic clouds causes a local increase of the ionic strength. Therefore, the amount of water in this region is depleted and an osmotic pressure is developed. The diffusion of water into this region to equilibrate the concentrations causes the particles to repel. This repulsion is the reason for the apparent stability of the suspension.

3.1.2.1.2.3 *Total potential energy of interaction*

The repulsive forces acting between two particles were calculated by two Russian scientists, Derjaguin and Landau, as well as by two Dutch scientists, Verwey and Overbeek, almost at the same time in the 1940s. Hence the theory of interaction between electric double layers is referred to as DLVO theory (Fig. 3.1.4).

The DLVO theory states that the sum of the expressions for the attractive potential energy, V_A, and the repulsive potential energy, V_R gives the total interaction energy V_T

$$V_T = V_A + V_R \tag{5}$$

3.1.2.1.2.4 *Electric double layer stabilization*

As the double layers of two approaching colloidal particles with the same charge start to overlap, the repulsion between them opposes the van der Waals attraction. If the repulsive potential is large enough to overcome the attractive van der Waals potential, it leads to electric double layer stabilization.

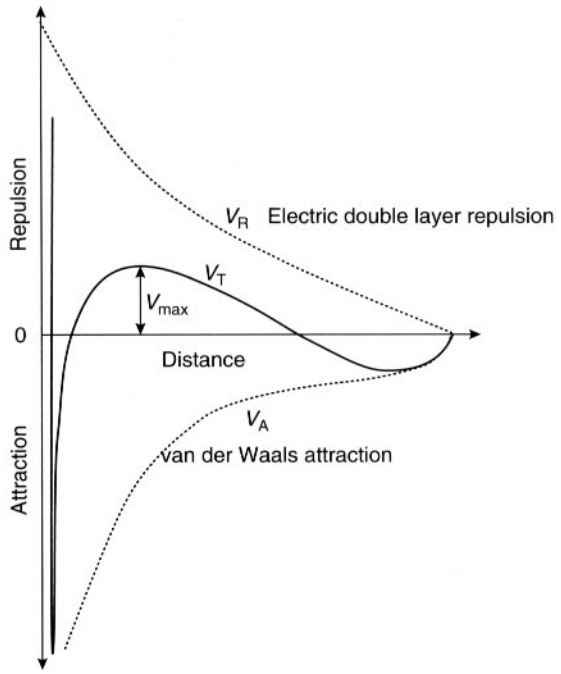

FIGURE 3.1.4 Potential energy between two particles in a liquid medium due to van der Waals attraction and electric double layer repulsion.

3.1.2.1.2.5 *Steric stabilization*

Steric stabilization is based mainly on two mechanisms. When two particles with adsorbed polymers approach each other, the number on conformations that the polymer can assume decreases due to the presence of the other particle. This results in a loss of conformational entropy. Secondly, the concentration of the polymer increases in the region of overlap. This results in osmotic repulsion between the particles in the suspension, which leads to stabilization of the suspension.

3.1.2.1.2.6 *Electrosteric stabilization*

Stabilization of slurry can also be achieved by a combination of electrostatic and steric forces. This can be done in three ways (i.e. with the presence of a charged particle and a neutral polymer molecule, in the presence of a neutral particle and a charged polymer molecule, or in the presence of a charged particle and a charged polymer molecule). The presence of charged particles produces

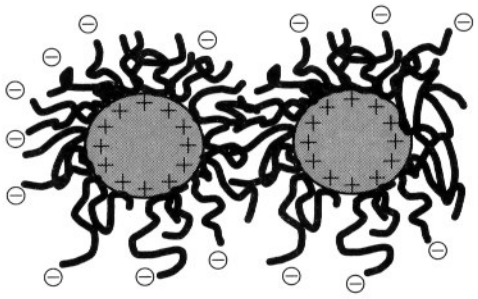

FIGURE 3.1.5 Schematic of electrosteric stabilization.

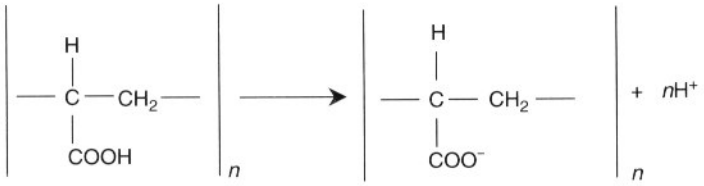

FIGURE 3.1.6 Dissociation of acrylic acid.

long-range repulsive potential and polymer molecules produce short-range repulsive potential as the particles approach one another (Fig. 3.1.5).

Polymer molecules have ionizable groups, which ionize in polar solvents, which give rise to a charged polymer. These polymers are called polyelectrolytes.

Figure 3.1.6 shows a schematic diagram of the dissociation of poly (acrylic acid) segments. The solvent conditions decide the fraction of dissociated functional groups. As the fraction of the dissociated functional groups, α, increases, the charge on the polymer varies from zero to highly negative or positive.

3.1.2.1.2.7 *Charge regulation*

At high concentrations, when the separation distances between the particles are very small (i.e. when it approaches 0), the repulsive pressure between the particles approaches infinity. Thus, the surface concentration of ions, which is proportional to the repulsive pressure P, also rises dramatically and approaches infinity [5, 6].

$$P = -\frac{\rho_s kT}{D} \tag{6}$$

$$\rho_s = \frac{2\sigma}{ze} \tag{7}$$

where σ is the surface charge density, ρ_s the surface concentration of ions, and D the separation distance between particles.

However, the infinite pressure is based on the assumption that, the surface charge remains constant. In practice, this is not so. When two particles are forced close to each other, the counterions are forced to adsorb onto their original sites. Hence, as D approaches 0, σ also falls. Hence, the surface potential remains constant. This effect is known as charge regulation. However, if there is no binding, the surface charge density remains constant and at the smallest possible separation distance, the counterion concentration approaches a constant value $2\sigma/eD$.

Thus, the charge regulation effect can be summarized as:

- The constant charge EDL repulsion is always higher than the constant potential EDL repulsion.
- Real surfaces show an intermediate behavior between constant charge and constant potential [6].

3.1.2.2 Coagulation

Most colloids are thermally unstable. They remain suspended only when the potential barrier is $\gg kT$. If the potential barrier is very small (i.e. $\ll kT$), particles come together and adhere. If this association is irreversible, the effect is called coagulation. If the adhesion between the particles is reversible, it is called flocculation. A *coagulate* is defined as a mass of particles adhered to each other due to van der Waals attraction formed in an aqueous suspension.

3.1.2.2.1 Kinetics of Coagulation

Particles in a suspension do not have a definite kinetic energy. At any given point in time, some particles may have higher energy as compared to others. The rate of coagulation is one of the most important characteristics of a colloidal suspension. The effect of DLVO theory on the kinetic behavior of particles in a suspension has been extensively studied [7]. The stability ratio W is given by

$$W = \frac{\text{Number of collisions between particles}}{\text{Number of collisions that lead to coagulation}} \tag{8}$$

and, the rate of slow coagulation is given by

$$R_s = W * R_f \tag{9}$$

where R_s is the rate of slow coagulation (when $V_T \gg kT$) and R_f the rate of fast coagulation (when $V_T \ll kT$).

3.1.2.2.2 Rate of Fast Coagulation

The rate of coagulation in the absence of repulsive barrier was addressed by von Smoluchowski [8]. He calculated the flux of a particle, which would come in contact with a fixed particle. The rate of fast coagulation is given as

$$R_f = 8\pi D a v_0^2 \tag{10}$$

where $D = kT/6\pi a\eta$ (m^2/s) (assuming uniform spheres), a is the particle radius (m), v_0 the initial particle concentration (number m^3), and η the viscosity of the dispersing medium (Pa s).

The time for the bulk concentration of the particles to reduce by half is given by

$$t^{1/2} = \frac{3\eta}{4kTv_0} \tag{11}$$

Smaller particles have faster coagulation rates as compared to larger particles.

3.1.2.2.3 Rate of Slow Coagulation

In the presence of energy barrier $\gg kT$, the rate of coagulation becomes orders of magnitude smaller than that calculated by Eq. 10. This potential energy barrier can be considered as activation energy for a coagulation event to take place. The equation for the rate of slow coagulation can be written as

$$R_s = \frac{8\pi D v_0}{\int_{2a}^{\infty} \left(\exp(V/kT)/r^2\right)\mathrm{d}r} \tag{12}$$

where V_T is the magnitude of the potential energy barrier and r the Distance from the particle center.

Substituting the values of R_s and R_f in Eq. 9, the value of stability ratio becomes

$$W = \frac{R_s}{R_f} = 2a \int_{2a}^{\infty} \exp\left(\frac{V_T/kT}{r^2}\right) \mathrm{d}r \tag{13}$$

This equation is solved numerically or graphically.

3.1.2.3 Rheological Properties of Suspensions

Rheology is the science of the deformation and flow of matter [6]. Rheology plays a very important role in the processing of the colloidal suspensions. Knowledge of rheological behavior can help characterize and optimize the

state of dispersion especially at high solids loading. This chapter discusses the fundamentals in and techniques useful for rheology.

Colloidal processing requires the suspension to have as high a solids loading and as low a viscosity as possible. Contrary to this the viscosity of ceramic suspension increases with the addition of more particles to the system. In order to achieve maximum solids loading with minimum viscosity, it is necessary to study the rheological behavior of the slurry so that its properties can be manipulated in order to achieve the above.

For liquids and suspensions, a characteristic property is used to describe the flow behavior, that is, *viscosity*. Viscosity measurements can be used as a method of analysis for determining the optimum solids loading of a colloidal system. By controlling the viscosity, it is possible to achieve optimum green body properties after forming. Viscosity can be defined as [9] (Fig. 3.1.7)

$$\eta = \frac{\tau}{\dot{\gamma}} \tag{14}$$

where τ is the shear stress, $\dot{\gamma}$ the shear rate, and η the shear viscosity.

Fluids are characterized by the way in which the viscosity changes with shear rate at a constant temperature. If the viscosity of the suspension is independent of the shear rate the fluid is said to exhibit Newtonian behavior (e.g. water). However, not all fluids exhibit Newtonian behavior. Colloidal suspensions are more often non-Newtonian in nature. Fluids in which the viscosity rises with the increase in shear rate are called shear-thickening fluids. This behavior is

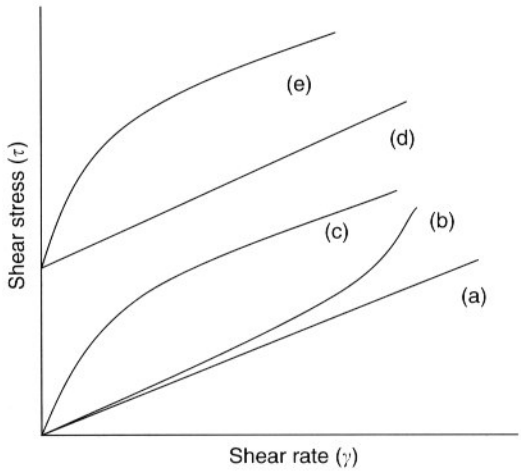

FIGURE 3.1.7 Typical rheological behavior of colloidal suspensions: (a) Newtonian; (b) shear thickening; (c) shear thinning/pseudoplastic; (d) Bingham; (e) shear thinning with yield stress.

exhibited by suspensions with a very high solids loading, which will eventually result in dilatancy of the slurry at very high strain rates. In some fluids, however, the viscosity decreases with increase in shear rate. These are called shear thinning or pseudoplastic fluids.

3.1.2.4 Parameters Affecting the Viscosity of a Suspension

3.1.2.4.1 Influence of Solids Loading on the Viscosity (Assuming Hard Sphere System)

For dispersions of non-interacting particles, the viscosity depends on the volume fraction of solids added to it. Increase in solids loading will cause an increase in the viscosity. Einstein proposed a method to describe this phenomenon. It is given by

$$\eta = \eta_s(1 + k_1\phi) \tag{15}$$

where η is the viscosity of the suspensions, η_s the viscosity of the suspending medium, k_1 the Einstein coefficient, which is equal to 2.5 for spheres, and ϕ the volume fraction of solids in the slurry.

This equation does not take into account the influence of particle size. Hence, this theory holds good only when there is no interaction between the suspended particles. Thus, this equation is valid only for dilute suspensions. When the system involves interaction between the particles (i.e. in case of concentrated suspensions) the situation becomes more complex and then the contributions due to particle interactions must also be included. This can be accounted for by including higher-order terms of ϕ. Thus, the extended Einstein equation is given as

$$\eta = \eta_s(1 + k_1\phi + k_2\phi^2 + \cdots) \tag{16}$$

A convenient way of expressing the viscosity of slurry is by dividing the slurry viscosity η_s, by the viscosity of the suspending media, η_l. This is a dimensionless quantity called the relative viscosity η_r. Increasing the volume fraction of the solids causes an increase in viscosity higher than that predicted by the power law expansion.

Thus, the effect of volume fraction of solids on the viscosity behavior is best studied in relation to the maximum packing fraction. With the addition of more and more particles, a stage is reached when the particles are jam-packed resulting in a continuous three-dimensional contact between the particles

throughout the system. This leads to immobilization of the fluid. At this point, when no flow takes place, the suspension is said to have maximum packing fraction ϕ_m.

In Refs [10, 11], a model for hard spheres is introduced. The equation for this model is given by

$$\eta_r = \left(1 - \frac{\phi}{\phi_m}\right)^{-[\eta]\phi_m} \tag{17}$$

where $[\eta]$ is the intrinsic viscosity.

However, this model applies only to monosize spheres. It does not take into consideration the particle size distribution of the powders. For data analysis of soft-sphere systems typically the high shear rate viscosities are taken into consideration for the calculations. This is because, at high shear rates the viscosity is dominated by the hydrodynamic force acting on the suspension.

3.1.2.4.2 Effect of Particle Size Distributions on the Viscosity of a Suspension

Most commercial ceramic powders have a continuous particle size distribution. The effect of particle size distribution on the viscosity becomes pronounced only at very high solids loading close to the maximum packing fraction of the suspension. Typically, the viscosity of polydisperse systems is lower than monodisperse systems at the same volume fraction, as the interstitials between the larger particles can be occupied by the smaller particles present [12]. Also, as the Krieger–Dougherty equation (17) suggests, the viscosity of monodisperse suspensions reaches a very high value at low solids loading. However, there is an optimum ratio in which the different particle sizes must be present. If a dispersion comprises of a higher fraction of the smaller particles, it may exhibit a lower maximum solids loading, thixotropy or plasticity. This occurs because of the increase in specific surface area able to bind more water and dispersant which would otherwise be available as dispersion liquid to yield a flowable dispersion. In case of dispersions with a high percentage of large particles, dilatancy is observed which obstructs flow. This lowers the maximum solids loading. When a high percentage of medium size particles are present in the dispersion, the particle size distribution becomes very narrow. The dispersion behavior approaches that of monodisperse systems. This again lowers the value of maximum solids loading due to trapping of water in the interstices of the large particles, which would otherwise be available for flowable dispersions [13] (Fig. 3.1.8).

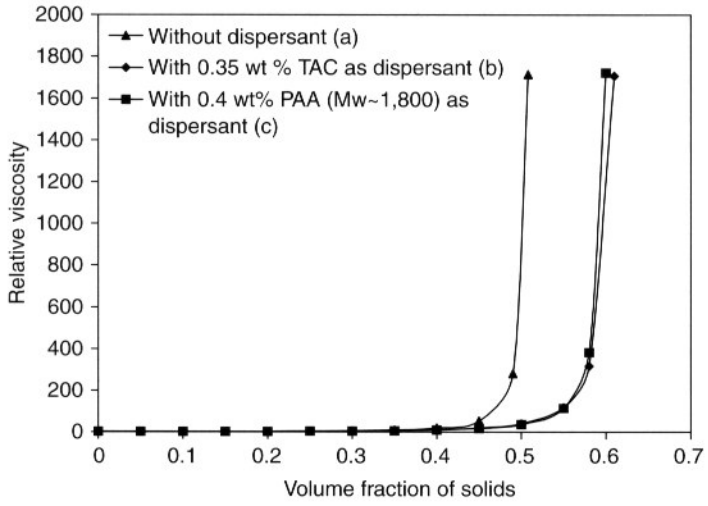

FIGURE 3.1.8 Dougherty-Krieger plots for alumina slurries: (a) stabilized by electric double layer; (b) electric double layer with short range repulsion from citrate anions; (c) electrosteric stabilization caused by poly (acrylic acid). Major differences in maximum solids loading are caused by agglomeration and subsequent solvent trapping.

3.1.2.4.3 Variation of Viscosity with pH

The pH of the suspension has a significant effect on the suspension viscosity. In case of oxides, the viscosity also indirectly varies with the zeta potential [9]. Viscosity of alumina slurry increases with increase in pH up to a certain value. Beyond a certain pH value the viscosity is inversely proportional to the suspension pH. The pH at which the viscosity reached a maximum value is the IEP of the suspension (Fig. 3.1.9).

3.1.2.5 Rheology of Sterically Stabilized Systems

In case of dispersions, which are stabilized by the addition of a polymer as a deflocculant, its rheology depends on three factors. They are

- The Flory–Huggins parameter χ. If the value of this parameter is less than 0.5, then the repulsion between the suspended particles will be strong enough for them to remain dispersed.
- The thickness of the layer of polymer adsorbed on the particles. The adsorbed layer thickness should be large enough to overcome the attractive van der Waals forces in order to prevent the particles from sticking

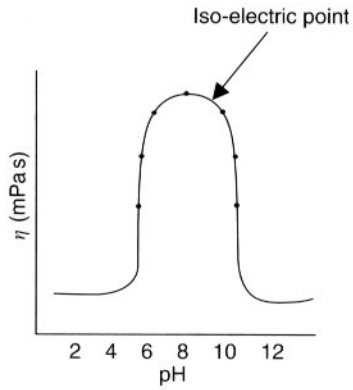

FIGURE 3.1.9 Schematic of effect of pH on the viscosity of alumina suspension.

to each other. The overlapping of the polymer layers is crucial as it is the prime cause of repulsion.

- The ratio of particle diameter to the adsorbed layer thickness [13]. The thickness of the adsorbed layer decreases with the increase in particle size. Hence, dispersions of small particles, due to large thickness of adsorbed dispersant layer tend to act like soft spheres.

3.1.2.6 Rheology of Electrosterically Stabilized System

Polyelectrolytes are widely used as dispersants for highly concentrated slurries (>50 vol%). They combine the principles of both electric double layer and steric stabilization. The effectiveness of electrosteric stabilization depends on pH and ionic strength as discussed in Chapter 2. At low solids loading (~20 vol%), the viscosity is relatively low and is affected very little by changes in viscosity. As the solids loading increases, the pH has a very significant effect on the viscosity. The amount of polyelectrolyte added also has a profound effect on the rheology of the suspension. The amount should be the optimum amount just enough to saturate the surface. Addition of higher than optimum amounts of polyelectrolytes results in excess amount of the polymer in the solution. The presence of the free polyelectrolyte in the solution can result in depletion flocculation, in case of high solids loading suspensions.

Conformation of the adsorbed polyelectrolyte also plays an important role in the rheological behavior of electrosterically stabilized slurries. The conformation in turn depends on the pH of the suspension. A detailed study of the adsorption behavior of poly electrolytes on Al_2O_3 [14, 15] shows that the

amount of polyelectrolyte adsorbed on the particle increases with a decrease in the pH value. When the pH increases to a value greater than the point of zero charge, the fraction of the polyelectrolyte dissociated is ~1. Hence, the negative charges in the polyelectrolyte repel each other. This reduces the loop formation in the conformation of the polyelectrolyte adsorbed on the particle surface. The polymer thus adsorbs in a extended conformation and the repulsion is short range. In this case, the stabilization is mainly due to the electrostatic forces. Conversely, at low pH values, the amount of polyelectrolyte dissociated and adsorbed on the particles surface decreases. As a result of this, the polyelectrolyte becomes uncharged. This favors the formation of the loop conformation of the polyelectrolyte segments. With thicker layer of adsorbed polymer with chains extending into the solution, the contribution of the steric forces towards stabilization is dominant [16].

3.1.2.7 Processing Additives

To overcome attractive van der Waals forces requires that additives have to be used in ceramic processing. Additives can have a wide variety and always have an impact on the particle–dispersing medium or particle–particle interfaces. Commonly, both organic and inorganic additives are used to improve the properties of the final ceramic green bodies and the sintered products [16]. For example, polymeric additives are used many times since they provide superior mechanical properties for handling. At the same time, polymeric compounds introduce specific problems that are related to their size.

In the dry powder direct compaction process, fine ceramic raw powders are processed into granules by adding organic binders to control the packing uniformity of the consolidated body, and the granule is made up of hundreds of fine raw powder particles. In theory, these granules are assumed to be perfectly homogenous distributions of particles and binder. In reality, granules might be hollow or show strong gradients of binder and fine particles enriched on the surface.

When dispersing ceramic powders in the solvent, dispersants are introduced to make a highly loaded suspension stable by adjusting the interparticle forces. While in tape casting or injection molding, the selection of suitable additives is one of the most vital steps. The following section will give a brief description of the commonly used additives according to their serving functions.

3.1.2.7.1 Dispersants or Deflocculants

In wet powder processing, a number of fundamental interactions can be used to alter the interparticle forces [16–19]. These forces include attractive van

der Waals forces, repulsive EDL forces, attractive or repulsive steric forces, and attractive capillary forces. EDL forces arise when solute ions or charge carrier function groups are attracted to or dissociation of soluble ions from particle surfaces occurs. Steric forces are developed by macromolecules that are attached to the surface of the particle. While charged macromolecules, that is, polyelectrolytes produce repulsive electrosteric forces [20]. Combination of the attractive van der Waals interaction and the repulsive double-layer repulsion is the foundation of the well-known DLVO theory, which provides an overall net interaction energy [18].

The attractive forces can be altered by changing the dispersing medium. The strongest impact on the van der Waals interaction range can be achieved by switching from high dielectric solvents to low dielectric properties.

The general explanation of the particle surface charge mechanism in the polar solvents is attributed to the accumulation of ionic species at the interface [16, 20]. The relationship between suspension microstructure, interparticle potential energy and the suspension structure can be schematically shown in Figure 3.1.10 [16].

Dispersants can be low molecular weight organic chemicals that carry functional groups for anchoring on surfaces and a buoy moiety. The buoy part is best if additional highly polar groups are available especially carboxylic acid groups as those develop negative surface charges in protic dispersing media

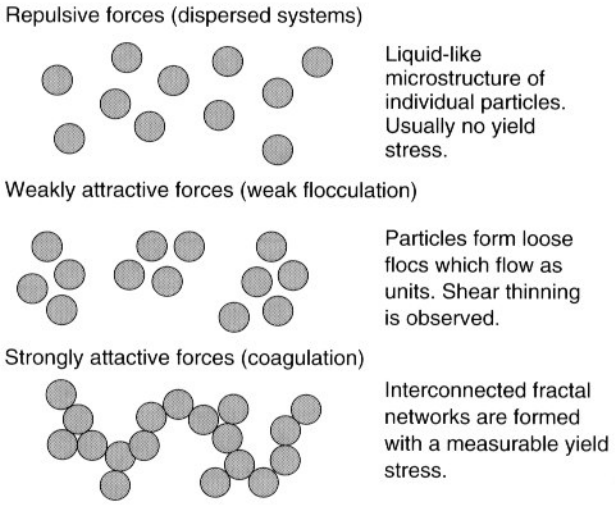

FIGURE 3.1.10 Schematic of the connection between suspension microstructure, interparticle potential energy and the suspension structure (from Ref. [16]).

above pH 3. Typical examples are citric acid or maleic acid. Other organic dispersants include polymers and poly electrolytes with molecular weights from 2000 for highly charged poly electrolytes and 100 000 for polymers. The size and the required charge of a successful dispersant can be predicted based on the particle size, the dispersing medium, that is, the main parameters controlling the van der Waals forces. In general, the repulsive barrier has to be close to or above $-0.5\,kT$ in order to have the Brownian energy to move the particles out of the attraction to achieve free flow.

Typical polar or dissociable functional groups for dispersant are hydroxyl (—OH), carboxyl (—COOH), sulfonate ($-SO_3^-$), sulfate ($-OSO_3^-$), ammonium ($-NH_4^+$), amino ($-NH_2$), imino (—NH—), and poly oxyethylene ($-CH_2\ CH_2O-$) groups (Fig. 3.1.11). Steric stabilization is the main contribution from these non-ionic macromolecules in the solid/solvent systems. The higher efficiency of the steric stabilization is realized by non-ionic macromolecules as compared to low molecular weight compounds [19]. Some commonly used dispersants are shown in Table 3.1.2.

The effect of dispersants can be strongly influenced by the solubility of the ceramic material. The solubility of ceramic materials is finite and covers many orders of magnitude depending on the material and the pH of the dispersing media. Increased solubility will cause an increase in counterions which will compress the electric double layer. Under these conditions

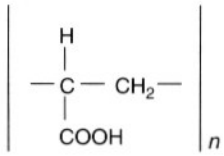

FIGURE 3.1.11 Schematic of polyacrylic acid.

TABLE 3.1.2 Commonly Used Dispersants in Ceramic Processing

Low molecular weight	High molecular weight
Sodium borate	Poly(acrylic acid) (PAA)
Sodium carbonate	Poly(methacrylic acid) (PMAA)
Sodium pyrophosphate	Ammonium polyacrylate
Sodium silicate	Sodium polyacrylate
Citric acid	Polyisobutene
Ammonium citrate	Menhaden fish oil
Sodium citrate	Phosphate ester
Sodium tartrate	Sodium polysulfonate
Sodium succinate	
Glyceryl trioleate	

a purely EDL-stabilized system will collapse. Sterically stabilized systems will also change since the solubility and conformation of polymers depends on ionic strength. Polymers might be salted out, that is, the suspension will coagulate. These mechanisms sometimes occur unwanted in processing or may be especially designed as part of a process as in the direct casting or constant volume techniques. An excellent source for understanding the solubility of ceramic materials is Mesmer's book *The Hydrolysis of Cations* [21].

3.1.2.7.2 Binders

Dry ceramic particle networks are very brittle and have very low strength, typically less than megapascals in compression. The only way to improve handling is to introduce materials that offer a toughening and strength increase, but also can be burned out. Therefore, polymeric materials are introduced. Typically, the addition of binder to the ceramic/solvent system is necessary to provide high strength to the green tape in the tape casting process after the solvent has evaporated [23]. During the granulation of fine powders, such as in spray drying, organic binders provide sufficient strength to bind hundreds of fine particles to form large (>50 μm) agglomerates and a free-flow powder [17]. The binder is a temporary bonding media for the powder particles and should give the green body a good handling and storage characteristics but should not result in cracks, pinholes and other defects in the unfired and fired parts. Table 3.1.3 gives typical recipes for spray granule additives, and Table 3.1.4 shows some typical data for industrially produced granules. In some colloidal processing, for example, tape casting, organic binder increases the viscosity and causes the change of the flow characteristics of the slurry. Moreover, binder, dispersant, and other additives in the ceramic mixture must be compatible with each other so as to avoid phase separation during the evaporation of the dispersing medium. A high molecular weight and a low glass transition temperature are advantageous. The binder must decompose into volatile products without residues of ash and carbon during the burnout process [22]. Table 3.1.5 lists the properties of some commonly used binder materials.

TABLE 3.1.3 Typical Recipes for Spray Granule Additives

Additive component	Vol.%	Type
Poly(vinyl alcohol) (PVA)	83.1	Binder
Glycerin	8.3	Plastisizer
Ethylene glycol	4.1	Lubricant
Dispersant	4.1	Dispersant
Non-ionic wetting agent	0.2	Dispersant
Defoamer	0.2	Defoamer

TABLE 3.1.4 Typical Data for Industrially Produced Granules

Granules	Primary particle size (μm)	Organic additive (vol. %)	Granule size (μm)	Granule density (%)	Tap density (%)
Al_2O_3 (substrate)	0.7	3.6	92	54	32
Al_2O_3 (spark plugs)	2.0	13.3	186	55	34
ZrO_2 (sensors)	1.0	10.5	75	55	37
Mn–Zn ferrites	0.7	10.0	53	55	32
SiC	0.3	20.4	174	45	29

TABLE 3.1.5 Commonly Used Binders in Ceramic Processing

Binders	Soluble in water	Soluble in organic solvents	Viscosity grade (effect to change the solvent viscosity)	Biodegradable
Poly(vinyl alcohol)	✓		Low–medium	
Poly(acrylic acid)	✓		Medium–high	
Polyacrylamide	✓		High	
Poly(ethylene oxide)	✓		Low–medium	
Polyethylenimine	✓		Low–medium	
Poly(methylacrylic acid)	✓		Medium–high	
Polyvinylpyrrolidone	✓		Low	
Methylcellulose	✓		Low–high	✓
Hydroxypropylmethylcellulose	✓		Low–high	✓
Hydroxyethylcellulose	✓		Low–high	✓
Sodium carboxymethylcellulose	✓		Low–high	✓
Ethyl cellulose		✓	Medium–high	
Starches	✓		Low–medium	✓
Dextrins	✓		Very low	✓
Sodium alginate	✓		High	✓
Ammonium alginate	✓		Very high	✓
Poly(vinyl butyral)		✓	Medium–high	
Poly(vinyl formol)		✓	Medium–high	
Poly(methyl methacrylate)		✓	Medium–high	
Polysilazane		✓	Medium–high	
Gum arabic	✓		Very low	✓
Guar gum	✓		Very high	✓

3.1.2.7.3 Plasticizers

Most binders require the addition of plasticizers to improve the flexibility and workability of the dried green body, such as tape. The choice of plasticizer is affected by compatibility, efficiency and stability. External plasticizing is

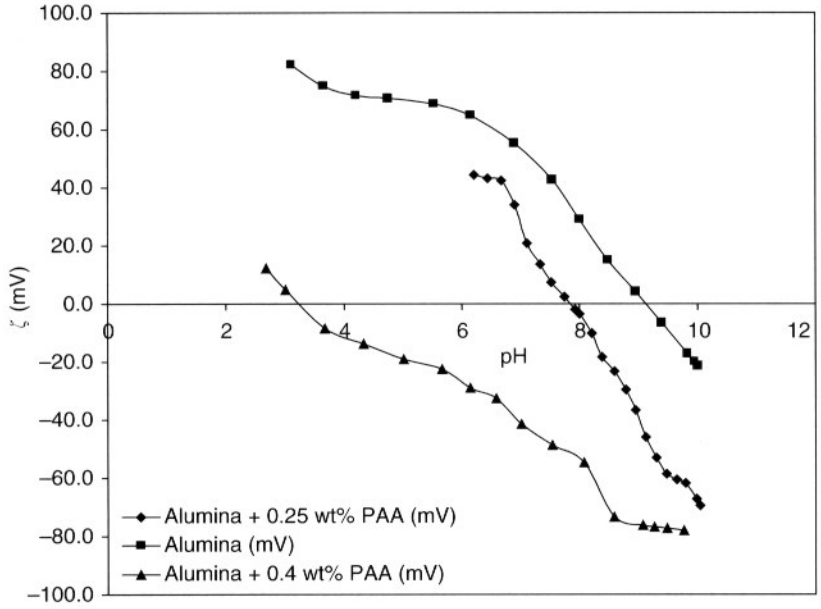

FIGURE 3.1.12 Shift in the isoelectric point of RC-LSC3DBM due to adsorption of polyacrylic acid $M_w \sim 1800$ on the surface of alumina particles. The amounts of PAA added are 0.25 and 0.4 wt% of alumina powder.

widely used, which means that binder polymers are mixed with low molecular weight plasticizers (M_w~300–400) or with oligomers in the M_w range of 3000–4000 [6]. Most widely used plasticizers are either glycols or phthalates such as polyethylene glycol or dioctylphthalate [23]. The principal function of plasticizers is to increase the chain mobility of binder molecules. With the optimal concentration of plasticizer, the intermolecular forces between polymer chains are weakened and the interchain distance between polymers, the intermolecular mobility is increased. Therefore, plasticization yields a decrease of the glass transition temperature of the softened polymer. Plasticizers are usually lower molecular weight organic compounds with a high boiling point, and they must be soluble in the same solvent used to process the binders (Figs 3.1.12 and 3.1.13).

3.1.2.7.4 Lubricants

Lubricants are commonly used in extrusion and injection molding to reduce friction between the particles or between the particles and the die wall. Stearic

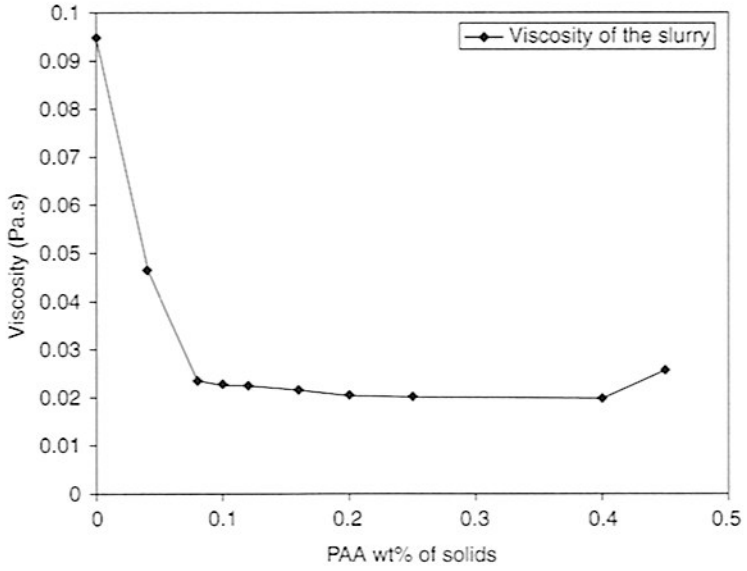

FIGURE 3.1.13 The amount of PAA $M_w \sim 1800$ required for lowest viscosity of aqueous slurry is in between 0.1 to 0.4 wt% for the here presented alumina powder at pH 9.

acid, stearates, and various waxy substances are commonly used lubricants. Table 3.1.6 shows some examples of the combination of the organic additives used in industrial pressing powders [4, 9, 23–26].

3.1.3 FORMING TECHNIQUES

3.1.3.1 Casting Techniques

3.1.3.1.1 Drained Casting

The drained casting techniques rely on phenomena that lead to separation of the liquid and solid constituents of a ceramic suspension on a macroscopic scale. The common goal with all approaches is to consolidate particles into a green body with desired shape and a mechanical strength sufficient for mold removal and handling.

Various techniques for liquid phase removal have been developed in the past. In slip casting, the solvent is drained by flow through porous walls of the mold. Capillary forces that depend on the pore size, a, and the surface tension at the liquid–vapor interface, γ_{LV}, give rise to a pressure gradient in the liquid that

TABLE 3.1.6 Some Examples of the Combination of the Organic Additives Used in Industrial Pressing Powders

Product	Solvent	Binder	Plasticizer	Others
Alumina	Acetone	Polyvinyl alcohol (low viscosity)	Polyethylene glycol (PEG) ($M_w \sim 400$)	Mg stearate (lubricant)
	Trichloroethylene (TCE)/ethanol	Polyvinyl butyral (PVB)	Poly(alkylene glycols)	Menhaden fish oil (dispersant)
Alumina substrates	Water	Polyethylene glycol ($M_w \sim 20000$)	None	Talc, clay (lubricant)
Alumina spark plug insulation	Acetone	Microcrystalline wax emulsion	KOH+tannic acid	Wax, talc, clay (lubricant)
TiO_2	Toluol	Ethyl cellulose Methylabietate	Diethyl oxalate Triethylene glycol Dihydroabietate	
Al_2O_3/ZrO_2	TCE/ethanol	Polyvinyl butyral	Polyethylene glycol/ phthalates mixture	Glyceryl trioleate (dispersant)
Mullite/SiC_w	Methyl ethyl ketone (MEK)/TCE	Poly(ethyl methacrylate) Poly(methyl acrylate) Poly(methacrylic acid)	Benzyl butyl phthalate (BBP)	
Mn–Zn ferrites	MEK/TCE	Polyvinyl alcohol (low viscosity)	Polyethylene glycol ($M_w \sim 400$)	Zn stearate (lubricant)
Ba titanate	MEK/ethanol	Acrylic binder	PEG/BBP	Phosphate ester (dispersant)
Ceramic tile	Water	Clay	Water	Talc, clay (lubricant)
Hotel china	Water	Clay, polysaccharide	Water	Clay (lubricant)
Refractories	Water	Ca/Na, lignosulfonate	Water	Stearate (lubricant)
$La_xSr_{1-x}MnO_3$	Ethanol/toluol	PVB	PEG/octyl phthalate	Glyceryl trioleate

drives the liquid flow

$$P_C = -\frac{2\gamma_{LV}}{a} \tag{18}$$

Often the growth rate of the slip-cast layer perpendicular to the mold surface exhibits a parabolic decrease with time. This makes slip casting a comparably slow technique and less suitable if thick consolidated layers are required. Osmotic consolidation exploits the osmotic pressure in a ceramic suspension that is in contact with a polymer solution via a semi-permeable membrane. Here, the difference in chemical potentials forces the solvent to flow through the membrane into the polymer solution. The resulting osmotic pressure can be defined as

$$\Pi = \frac{\mu_S - \mu_P}{V_m} \tag{19}$$

where μ_0 is the chemical potential of the solvent in the ceramic suspension, μ_P the chemical potential in the polymer solution, and V_m the molar volume of the solvent. Compared to the capillary pressures in slip casting, osmotic pressures are significantly higher. Alternatively, an external, mechanical pressure can be applied to the ceramic suspension, which drives the solvent through a filter membrane. This technique is known as filter pressing. Consolidation rates are comparably high for filter pressing because the employed pressures are usually about one or two orders of magnitude larger than typically encountered in slip casting. The flux of liquid through the porous particle layer is a function of the pressure gradient ∇P, the permeability D, and the liquid viscosity η according to Darcy's law

$$J = -\frac{D}{\eta}\nabla P \tag{20}$$

In tape casting, a ceramic suspension is deposited on a flat carrier substrate and the solvent is removed simply by evaporation. The rate of solvent removal is therefore mainly dependent on temperature, convective and diffusive solvent transport at the liquid–vapor interface, and internal capillary pressures in the porous layers of the cast tape.

Macroscopic separation of solid and liquid phases in a ceramic suspension can also be achieved with the help of body forces acting on the dispersed particles. Analogous to particle sedimentation caused by gravitational forces, centrifugal forces can be used to consolidate particles in a rotating mold. The settling velocity of a single spherical particle in the centrifugal force field can be approximated by a modified Stokes equation for particle movement in dilute suspensions

$$v = \frac{2\Delta\rho R^2\omega^2 z}{9\eta} \tag{21}$$

where $\Delta\rho$ is the density difference between solid and liquid, R the particle radius, ω the angular velocity, and z the distance from the rotation axis. One advantage of this method is the linear relation between cast layer growth and casting time, because no liquid has to be forced through a porous layer as in slip casting. Like in slip casting, cast bodies made by centrifugal casting can suffer from inherent density gradients. An electric field can be used in a similar manner to accelerate particles suspended in a liquid if the particles carry a surface charge. The corresponding technique used to consolidate particle into dense layers is called electrophoretic deposition. Similar to centrifugal casting, the accelerating force is balanced by viscous forces resulting in a steady state particle velocity

$$v = \frac{\varepsilon_r \varepsilon_0 \zeta E}{f_H \eta} \tag{22}$$

with ε_r being the relative dielectric constant, ε_0 the permittivity of free space, ζ the particle's zeta-potential, E the applied electric field strength, and f_H the Henry constant, which ranges from 1 to 1.5 depending on the particle size and ionic strength.

In suspensions with purely repulsive particle interactions, the consolidation pressure has to exceed the osmotic pressure of the ceramic suspension in order to achieve dense particle packing. The osmotic pressure of a hard-sphere system, Π, is a function of the solids volume fraction, Φ, namely

$$\Pi(\Phi) = \frac{RT\Phi(1 + \Phi + \Phi^2 - \Phi^3)}{V(\Phi_{max} - \Phi)^3} \tag{23}$$

where R is the gas constant, T the temperature, V the molar volume of the colloid phase, and Φ_{max} the maximum solids loading [27].

In suspensions with attractive interparticle forces, the applied pressure for consolidation has to exceed the yield stress of the space filling particle network. The relation between the yield stress, τ_Y, and the solids volume fraction can often be described by an empirical power law of the type

$$\tau_Y \propto \Phi^n \tag{24}$$

where n is a constant fitting parameter.

3.1.3.1.1.1 *Tape casting*

Liquid casting techniques allow for easy manipulation of the shape of a ceramic before sintering. Wet casting techniques involve molding a slurry—a mixture of one or more ceramic powders in a liquid, which can be either water or an organic solvent. Often other additives must be added to enhance the properties of the slurry during the casting process. Tape casting uses these principles of wet

casting originally used for drain casting in order to make thin ceramic tapes. Tape casting is a method for making thin, flat ceramics as small as a few microns.

Introduction and background

The main advantage of tape casting is the ease of use for producing thin, flat ceramic and metallic parts. These parts cannot be pressed. Only recent developments in extrusion allow similar qualities. Tape casting involves spreading ceramic slurry onto a table where the liquid is removed. Tapes can be cast from 1 μm to 1 mm thickness, depending on the desired application. The original purpose of this practice was for applications in electronics and radio, which is still the chief market today. Tape-cast products include dielectric capacitors, piezoelectric actuators, along with thick and thin films.

The patent for tape-cast ceramics was granted to Glenn Howatt in 1952, although the methods for this process had been researched extensively during the Second World War [28]. In 1961, a patent was awarded to the American Lava Corp. who developed a method to continuously cast ceramic tapes. This paved the way for large-scale operations and in-line processing. In the late 1950s and early 1960s, Warren Gyurk developed a way to use ceramic tapes to make multilayered laminates, such as with today's multilayered capacitors [29].

Today, the tape casting industry is looking for technological advances using the original techniques of Howatt and Gyurk. Powder particle sizes, which were once several microns, are now in the submicron range. This has produced considerable research into various slurry additives used to optimize the properties of the slurry. Thinner films are being developed, which means more refinements are being looked into modern processing equipment and materials. With these advances, many exciting, new technological frontiers will be reached in tape casting over the next number of years.

Slurry composition

Although shaping, binder burnout, and sintering are important stages in determining the final properties of a tape-cast part, the original slurry composition is the most important influence on the final product. The variables of a slurry for a tape casting run must be in the optimized for viscosity, particle size, and miscibility. In general, the desirable viscosity is 3000–5000 mPa s with a powder particle size of 0.5–2 μm. However, these properties vary depending on the main powder, casting speed and thickness, and final application.

Solvents/dispersing media

A common problem with almost all powders is that they are agglomerated. Therefore, the particles must be dispersed. In order for this to occur, and to

make a slurry, a solvent and a dispersant are added. The solvent is the medium for the slurry that gives it flow characteristics. A solvent must:

- dissolve other organic additives,
- have a low viscosity,
- be inclined to not foam,
- have a low boiling point,
- be non-reactive with the powder,
- be non-volatile and non-toxic.

The right solvent for a slurry has to meet all of the previous characteristics [23, 28] for the given powder. For example, an alumina system will use trichloroethylene as a solvent, whereas a $BaTiO_3$ system has mostly an ethylene system. These two systems are shown in Table 3.1.7. These are based on the colloidal chemistry of the individual powder and the other additives. Although water-based systems are currently being researched, water has a lower evaporation rate and higher polarity, and therefore the majority of tape casting systems still prefer non-aqueous systems. Generally, blends of an alcohol and an organic solvent are used. This allows the other additives to be dissolved in the solvent and keep the viscosity low during milling. Novel developments in green processing will allow avoiding organic solvents in the future.

Dispersants

The dispersant, also called a surfactant or deflocculant, are molecules or polymer chains adsorbed onto the powder particles. Dispersants are important to add to a slurry system so that the cast tape can be uniform and homogenous. Dispersion also helps provide uniform packing in the green body yielding uniform shrinkage during drying, binder burnout and sintering. Like with other additives, dispersants are system specific. However, Menhaden fish oil was found to be useful for a variety of non-polar systems. Menhaden fish oil is

TABLE 3.1.7 Compositions for Typical Tape Casting Slurries

Function	Composition [23]	Vol %	Composition [30]	Vol %
Powder	Alumina	27	Barium titanate	66
Solvent	Trichloroethylene	42	Ethanol	10
	Ethyl alcohol	16	Methylethyl ketone (MEK)	10
Dispersant	Menhaden fish oil	1.8	Menhaden fish oil	0.6
Binder	Polyvinyl butyral	4.4	Acryloid B-7 MEK	8.8
Plasticizer	Polyethylene glycol	4.8	Polyethylene glycol	2.6
	Octyl phthalate	4.0	Butyl benzyl phthalate	2.6
Homogenizer			Cyclohexanone	0.4

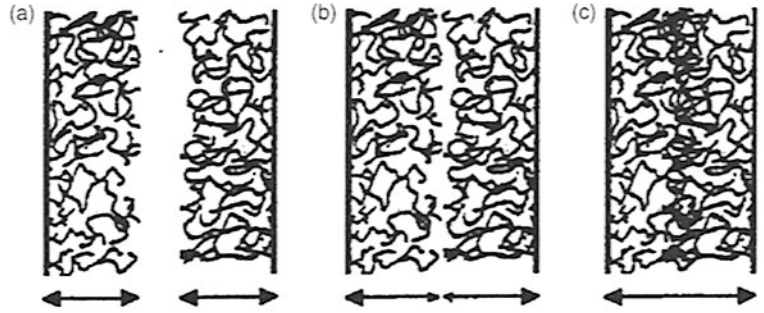

FIGURE 3.1.14 Steric interaction in polymer coated surfaces: (a) no interaction; (b) little repulsion; (c) penetration of polymer layers—strong repulsion.

highly purified non-drying oil derived from *Brevoortia tyrannus*, a herring like fish living off the Eastern coast of the United States. The oil is transformed into a useful dispersant for ceramic processing through auto-oxidation. This process causes a poorly controlled polymerization of the highly unsaturated triglycerides. The auto-oxidation is stopped after a certain viscosity has been reached. Menhaden fish oil for ceramic processing is a polydisperse polymeric (dispersity above 40, standard synthetic polymers are around 2) mixture having high molecular weight fraction above 100 000.

It still contains fatty acids, non-reacted triglycerides, and an intermediate molecular weight fraction. This multitude causes problems in processing due to the non-reproducibility of the oil and therefore its colloidal stabilizing ability. Synthetic substitutes have been developed. As with all dispersants complete surface coverage of the powder is required yielding low amounts of typically 1 wt% of dispersant (Fig. 3.1.14).

Binders

The purpose of the binder is to provide strength to the dried ceramic tape. This is important especially in storing and machining the dry tape. Since there is no other material group available to yield these properties organic polymers are introduced. The strength of polymers is derived from the size, that is, the molecular weight. The solubility of polymers in the dispersing medium and the viscosity of the polymer solution limit the size of the polymer. Therefore, binders are typically polymers with a molecular weight around 100 000. Since the binder is another polymer in the slip, the surface chemistry has to be tailored as well as the hierarchy in processing has to be kept in order to achieve the very well-defined nanostructure. Dispersants have to be added first to the slurry, then the binder. If they are added at the same time or reversed unfavorable

nanostructures on the surfaces are achieved that lead to flocculation and high viscosities.

The binder should:

- form a strong, cohesive tape when dried,
- be miscible or emulsifiable in the solvent,
- be inexpensive,
- readily burnout without leaving a carbon residue.

The polymeric properties [30] of the binder are important to allow the ceramic to maintain its strength and shape until firing.

Plasticizers

Most synthetic polymers have glass transition temperatures above room temperature. The brittle behavior of glasses is not useful for ceramic green tapes therefore the glass transition temperature of the polymers has to be lowered. This is most easily done by adding solvents with a low vapor pressure, or in other words, a high boiling point with typically above 250°C. These solvents are referred to as plasticizers. Adding too much plasticizer degrades the strength of the binder, which will also cause problems during machining. Therefore, the binder and plasticizer ratio much be carefully monitored to provide optimal properties for the tape. Generally, two different plasticizers are added to slurry although one suffices for the green tape. This tradition of using two might have a positive impact on drying and burnout.

Other additives

Several other additives can be used to enhance the final product. Wetting agents, or homogenizers, increase the solubility of the many liquids in the slurry. These wetting agents also contribute to high-quality tape surfaces. Cyclohexanone is a common homogenizer. Defoaming agents, such as dimethylsilicones, are used to prevent foaming and allow trapped air bubbles to escape easier on degassing. They commonly have to be used in aqueous slurries or when sub-micron powders are used. They work by removing surplus surfactants from the bubble surface, thus increasing the bubbles interfacial energy and making it unstable. However, the complexity of having many organic additives makes the prediction of the usefulness of the defoamer difficult (Figs 3.1.15–3.1.17).

Other tape casting techniques

Waterfall technique: Analogous to the glazing of ceramic tile, this casting technique involves using a pump to pour a curtain of slurry onto a substrate, which is then dried. The slurry "curtain" or waterfall must be kept

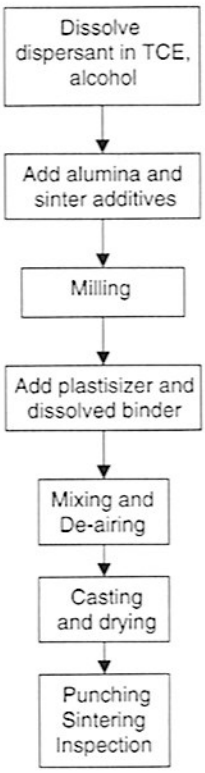

FIGURE 3.1.15 Flowchart for tape casting alumina substrates.

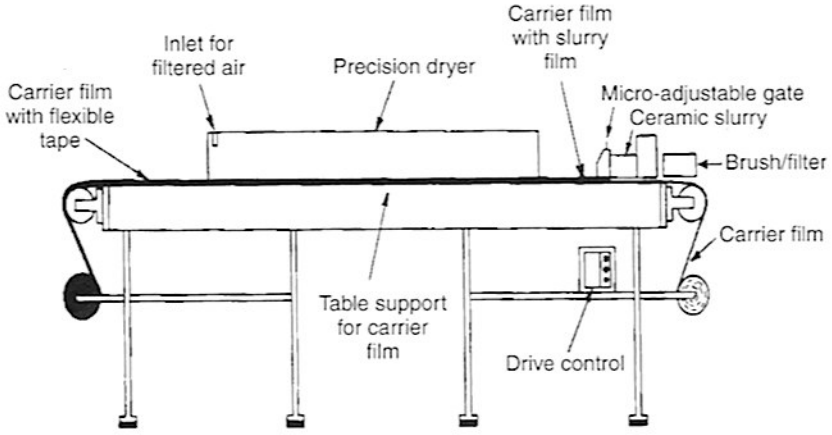

FIGURE 3.1.16 Diagram of a continuous casting machine (from Ref. [9]). This material is used by permission of John Wiley & Sons, Inc.

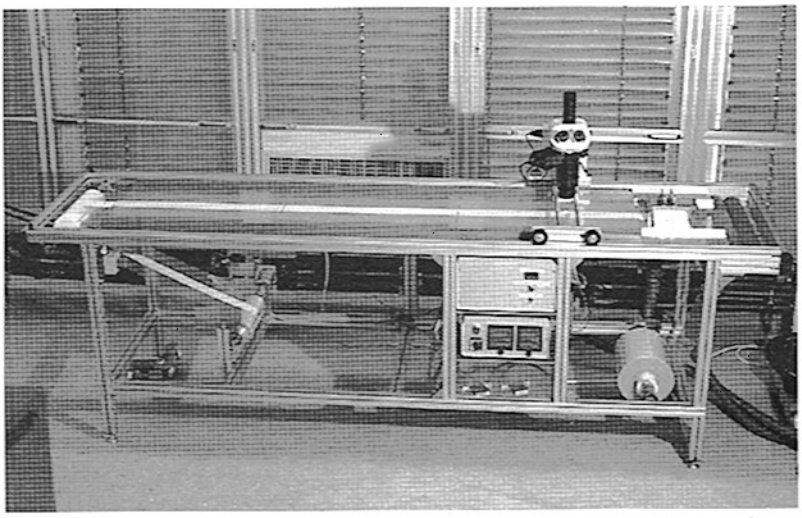

FIGURE 3.1.17 Laboratory scale tape caster for batch casting of ceramic tapes.

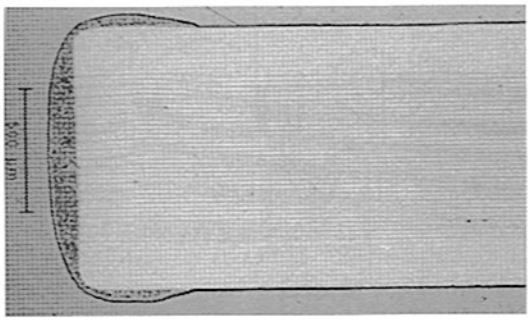

FIGURE 3.1.18 Polished long-transverse section of a multilayer capacitor.

thin and uniform to avoid splashing or other non-uniformities. This technique is used for making porous electrodes for fuel cells and multilayer ceramic capacitors [31] (Figs 3.1.18 and 3.1.19).

Paper casting: In this process, a low-ash paper is passed through slurry. The slurry sticks to the paper, which is passed through a dryer and rolled onto a reel (Fig. 3.1.20). The paper is removed during BBO. This process is used for honeycomb structures such as heat exchangers and catalytic converters [31].

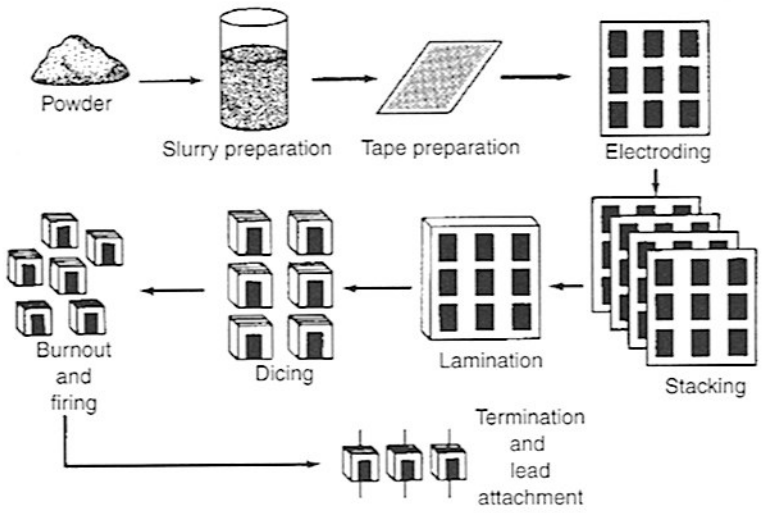

FIGURE 3.1.19 Steps for fabricating mutlilayer capacitors using tape casting (from Ref. [31]).

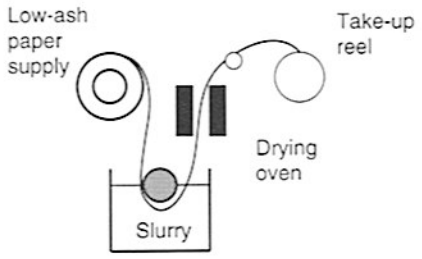

FIGURE 3.1.20 Schematic showing the paper-casting process.

Common problems and defects: All of the variables involved in tape casting must be carefully monitored and controlled to prevent defects in the final product, such as cracks, non-uniformity, delamination, and surface roughness. The majority of these problems can be traced back to the slurry composition. A common problem during casting is excessive sticking of the tape to the belt. Adding more dispersant and plasticizer will alleviate this problem. On the other hand, adding too much of both will cause the tape to release early from the belt and curl up. A weak tape is a sign of too little binder, just as a brittle tape is deficient in plasticizer. Even the smallest deviation in additive composition can greatly change how the tape and the final product turn out.

3.1.3.1.2 Constant Volume Techniques

3.1.3.1.2.1 *Gel casting*

Wet powder processing is conducted by dispersing ceramic powders in the solvent to form a highly loaded, while stable, suspension for the following consolidation. It is known that hard agglomerates limit uniform consolidation of green compacts of ceramics and results in defects in the final sintered parts. Since there are always soft agglomerates or hard agglomerates in the raw powders, de-agglomeration is needed to break them into individual particles. The aggregate structures of fine powders can be dispersed by adjusting pH and/or many types of dispersants in suspension, and sometime the efficiency can be enhanced by ball mill. Normally dispersant and other organic additives may be required to generate repulsive energy barrier to avoid flocculation. The suspension can then be cast into either a porous mold (slip casting) to consolidate the slip or a non-porous mold (constant volume casting) to induce flocculation by adjusting process parameters. After the wet green body is formed, it is demolded and drying is followed to get the dry green body. The up-to-date ceramic forming techniques through wet powder processing will be discussed in the following section.

3.1.3.1.2.2 *Extrusion*

Extrusion is a manufacturing technique for the production of long pieces of material with a common cross-section. The material is forced through a carefully shaped nozzle at high pressure to form a continuous length body. Extrusion is important in the manufacture of components from metals to ceramics and plastics. Highly ductile metals such as aluminum are extruded cold (at room temperature) to form hollow bars and tubes for low-strength applications such as window frames. Other metals such as copper and brass are extruded hot to form water pipes and pipe fittings. In the ceramics industry, extrusion is used to form square-section bars which can be cut into bricks, while viscous alumina slips are extruded into complex, thin-walled honeycombs, used as support media for catalysts. Thermoplastics become viscous on heating and can be extruded in many forms [4, 9].

In the manufacturing of ceramic green bodies by conventional extrusion, a ceramic paste is prepared by mixing ceramic powder with polymers and other additives first. Then a rotating screw, together with heaters, heats the material and continuously pushes this paste through a die with the shape of the profile to form a green ceramic string. After the die, the profile is cooled by air or water and cut into desired lengths. The advantages of the extrusion process are that profiles of all shapes can be made and production volumes are normally high. Water (traditional ceramics) or organic materials (technical ceramics) are added

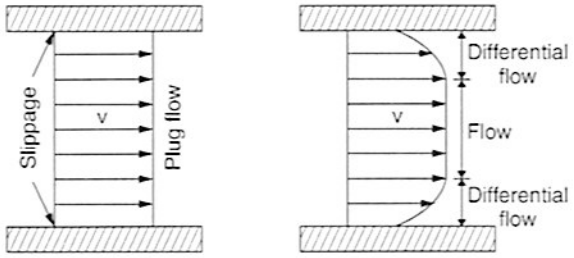

FIGURE 3.1.21 Cross-section velocity profiles for (left) plug flow with slippage at wall and (right) differential laminar flow near wall (from Ref. [9]). This material is used by permission of John Wiley & Sons, Inc.

to provide adequate plasticity for forming. The major difficulty is removing the organic material prior to firing, without causing cracks or distortions.

During extrusion, the driving force produced by the auger or piston must exceed the resistive force of the plastic material and the die–wall friction. The pressure motivating flow is highest in the barrel and decreases along the axis of the extruder. The particular flow behavior depends on the geometry of the die and the flow properties of the materials. Figure 3.1.21 shows the cross-section velocity profiles during extrusion.

In conventional extrusion, the fabricated object takes the cross-sectional shape of the extrusion die and can be no smaller than the die orifice. Use of co-extrusion for microfabrication (MFCX), which is a new method to produce axis-symmetric ceramic objects with micrometer-size feature in two dimensions, has also been reported. The MFCX process uses simple round or square dies for size reduction. Shaping is done by using a shaped object of two or more materials as the extrudate. One material is the primary ceramic plastic compound, the ceramic which is to be microfabricated. The second material is a fugitive substance, whose function is to fill space and have similar flow behavior as the primary material during extrusion. These are extruded together, or co-extruded, to reduce the cross-sectional dimensions. The fugitive material is later removed. This method can be used to produce several shapes in alumina and PbO-containing ferric ceramics with carbon black, removed by oxidation, as fugitive. Composites with layers as fine as 8 μm have been made with this process [32–34].

Figure 3.1.22 shows schematically the geometry of the ceramic composites that can be microfabricated by co-extrusion.

3.1.3.1.2.3 *Injection molding*

Injection molding techniques are frequently employed to produce ceramic parts with complex shapes that are difficult or even impossible to realize with

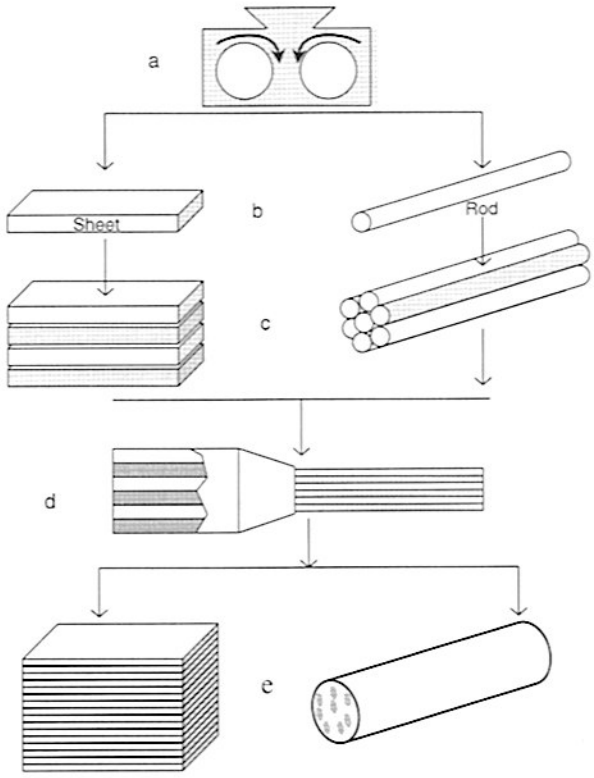

FIGURE 3.1.22 Piezoelectric ceramic/polymer composite formed by co-extrusion: (a) compounding powder; (b) performing; (c) lamination; (d) extrusion; and (e) 1–3 composite.

many other forming techniques. Moreover, when using injection molding, it is comparably easy to switch the production to a different product simply by exchanging the mold and feedstock.

Basically, the feed material consists of a mixture of one or more ceramic powders and a polymer or wax as a binder phase. Additionally, dispersants and plastisizers may be added to enhance flowability of the mix and to prevent agglomeration of the particulate phase. The feed material is fed into a heated chamber in order to soften or liquify the binder, which is necessary for optimum mold filling. The filling of the mold is usually accomplished by the action of a plunger or a screw that forces the feed material through a nozzle into the mold cavity. After mold filling is completed, the material is allowed to cool down until the binder solidifies. Then, the mold can be opened and the ceramic part ejected.

The factors that may limit the use of injection molding techniques are related to cost competitiveness and difficulties to produce large parts. The design of an

injection molding machine has to take account of the high pressures created during an injection cycle. Moreover, precise control of the mass of the injected material, of the materials temperature, and of the position of the plunger or screw is essential for the manufacturing of high-quality parts. Wear of the surfaces that come in contact with the highly abrasive feed material is another factor that increases the costs of injection molding processes. Binder formulation is crucial for the quality of injection molded parts [4].

Suitable rheological properties of the feed material are required during mixing and injection. This means that the injected material must have a sufficiently low viscosity at relevant shear rates and temperatures. Accordingly, not only the binder viscosity must be low but also the solids fraction of the feedstock needs to be well dispersed in the binder matrix phase. Furthermore, viscoelastic properties of the feed material have to be considered; for example, time and temperature-dependent relaxation of shear stresses after mold filling might lead to unwanted dimensional changes. Binder properties are also of considerable importance in subsequent processing stages; for example, burn-out behavior of the binder can pose limitations on the geometry and the dimensions of the ceramic part [35].

3.1.3.1.2.4 *Pressing (die, CIP)*

Dry powder processing involves the direct compaction of either the raw fine particles or the granular powders in a rigid die. The commonly used methods are die pressing, cold isostatic pressing (CIP), hot pressing (HP), and hot isostatic pressing (HIP). Die pressing is widely used to produce simple-shaped engineering parts because it can be easily automated. HP and HIP can make the forming of the green body and sintering possible at the same time, but they require specific apparatus. These consolidation techniques will be described in the following sections.

Die pressing

Die pressing is conducted by applying stresses directly in a vertical direction to the granules of ceramic powders that are loaded in a mold to generate loose bonding between powders so that the compact can have some mechanical strength to be handled. During die pressing, the shape of the ceramic powder granule changes (illustrated schematically in Figures 3.1.23 and 3.1.24), which comprises three steps: (a) packing of granules; (b) deformation of granules; and (c) sliding in between the granules so that the size of the voids between the deformed granules can be decreased.

When the stress or force is applied only from one side, for example, from the upper side of the mold (Fig. 3.1.25), this die pressing is referred to as uniaxial pressing. The advantage of this process is fast and easy automation,

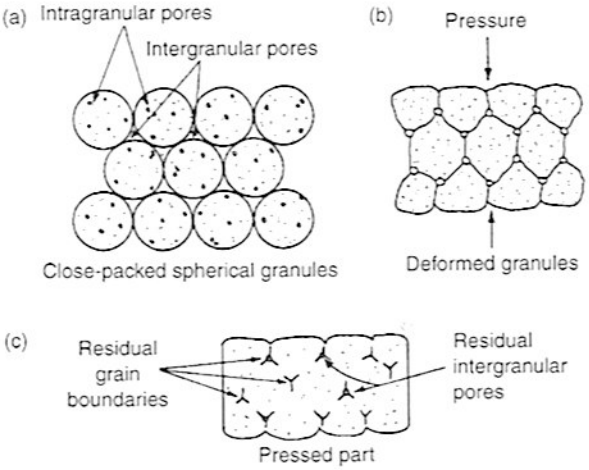

FIGURE 3.1.23 Change of granule shape on pressing: (a) packing of granules; (b) deformation of granules; (c) sliding in between the granules (from Ref. [9]). This material is used by permission of John Wiley & Sons, Inc.

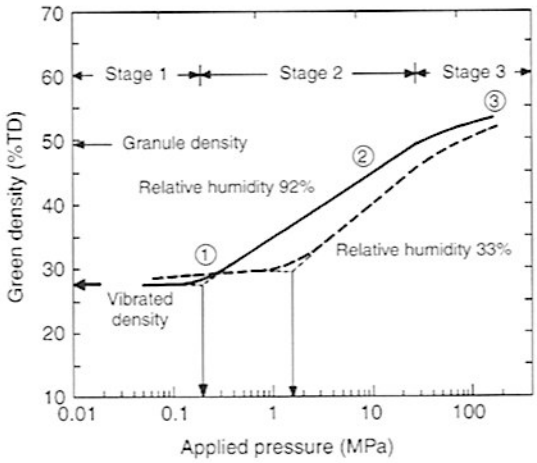

FIGURE 3.1.24 Compaction states while pressing: (1) packing of granules; (2) deformation of granules; (3) sliding in between the granules (from Ref. [9]). This material is used by permission of John Wiley & Sons, Inc.

but the shortcoming is the stress gradient that may result in density gradient in the compact green body. Sometimes lamination may also occur because of the inhomogeneous distribution of the applied stress, and some typical flaws in pressed parts.

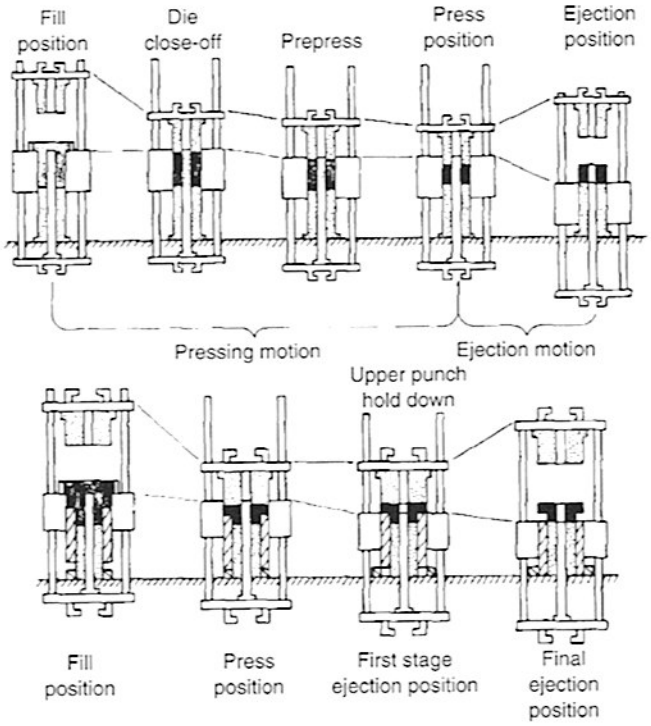

FIGURE 3.1.25 Press and ejection movements for different press matrices (from Ref. [9]). This material is used by permission of John Wiley & Sons, Inc.

To minimize the above problem, the stress can be applied from both upper and bottom directions, this is called biaxial pressing. For very large parts, there is still a problem of density gradient, especially in the areas along walls of the mold because of frictional resistance.

Cold isostatic pressing

CIP utilizes the hydrodynamic forces through liquid media to apply the stress to the powder compact in all directions, therefore, it can be used to form parts with only one elongated dimension, relatively complex, or those that may not easily be die-pressed. Typically, CIP may be divided into wet-bag and dry-bag type CIP. In the wet-bag process (Fig. 3.1.26), the powder is filled into a mold first and then the stress or force is applied in all directions. Operating pressures up to 200 MPa are commonly employed and wet bag presses operating to 500 MPa are used for pressing large blocks. This requires that the rubber mold filled with ceramic powders be immersed in a liquid media. Then the force applied to the liquid media can be passed on to the rubber mold and the force is the

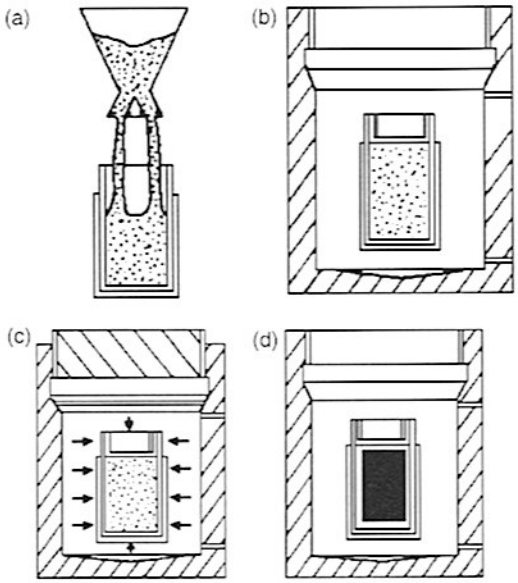

FIGURE 3.1.26 Schematic of the CIP process: (a) telling of powder; (b) installation of mold; (c) isotactic pressing (d) removal of mold (from Ref. [9]). This material is used by permission of John Wiley & Sons, Inc.

same in all directions. Therefore, the ceramic compact green body will have less density gradient. But this method encounters problems when the part is too complicated and/or the surface finish is not good. As a variation of the wet-bag CIP, in the dry-bag processing, the forces are only applied radially through the pressurized liquid medium between a flexible mold and a rigid shell, as is shown schematically in Figure 3.1.27. Therefore, this process can be used to automatically produce ceramic parts.

Hot pressing

Compared with CIP, HP is more complex and requires special apparatus (Fig. 3.1.28). It renders the compaction of powders and the sintering of green body at the same time. A mechanical pressure (> 20 MPa) increases the sintering driving pressure for densification by acting against the internal pore pressure without increasing the driving force for grain growth. Therefore, sintering temperature can be reduced and a relatively finer microstructure and higher density can be obtained. HP is commonly used to sinter a high-purity product that requires very high sintering temperatures under normal atmospheric pressure and sintering aids are thought to cause drastic influence on the mechanical properties under the actual serving environment. Another variation of HP is HIP, which uses hot pressurized gas in the range of 10–200 MPa as

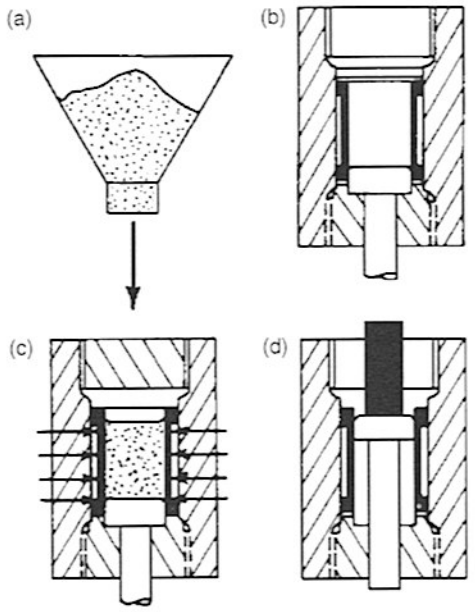

FIGURE 3.1.27 Dry-bag pseudo-isopressing—simplified automatic variation of CIP: (a) powder filling; (b) open mold; (c) pseudo-isotactic pressing; (d) ejection of part after decompression (from Ref. [6]). This material is used by permission of John Wiley & Sons, Inc.

the medium to apply the external pressure to the sintering compacts. HP or HIP can also be used as a post-sintering technique to reduce the size of the closed pores. Similar to the CIP technique, the shape of the product should not be very complicated. The size of the part is also limited because of the dimension of the chamber inside the apparatus.

3.1.4 DRYING

A crucial task in the drying process of ceramic green bodies is the minimization of non-uniform drying stresses in order to prevent cracking, non-uniform deformation, or the formation of density gradients in the green body structure. The development of non-uniform drying stresses has been related to pressure gradients in the pore liquid and in the vapor phase of unsaturated pore space, and to temperature gradients that cause differential thermal expansion [36, 37]. The evolution of the pressure and temperature distribution in a porous body is dependent on several transport phenomena such as diffusion of solvent molecules, liquid flow, and the conduction of heat. Interparticle

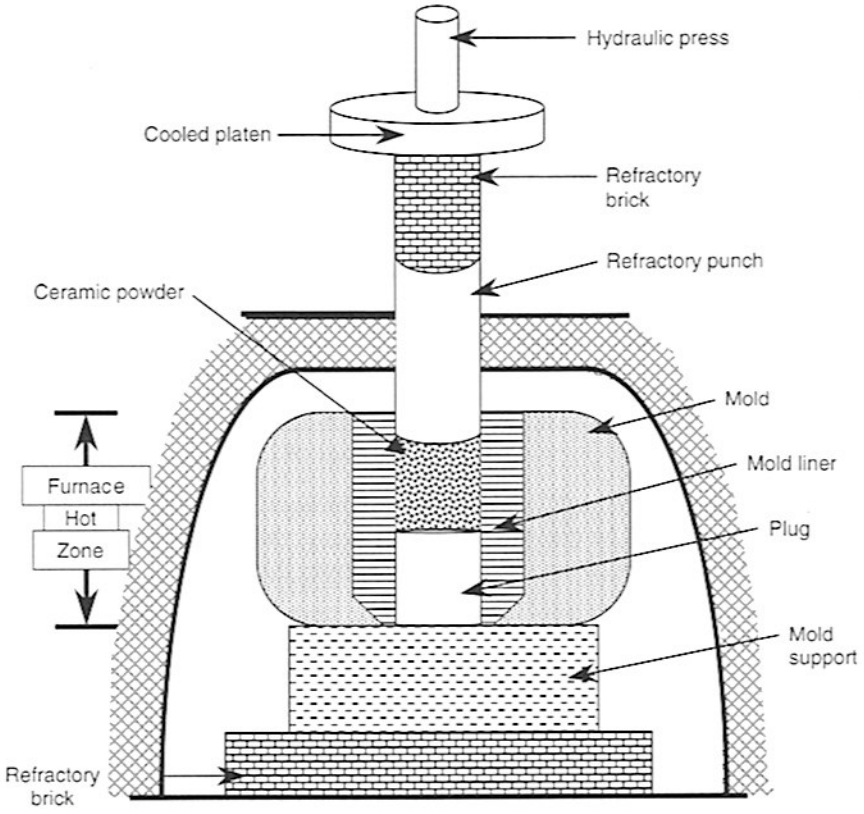

FIGURE 3.1.28 Schematic drawing of a hot press furnace (axial pressing in a furnace at up to 2000°C).

forces, friction forces, and the resulting viscoelastic properties of the particle network determine deformation and particle rearrangement in response to the mechanical drying stresses.

In ceramic processing, the shrinkage of a green part during drying is usually caused by capillary phenomena due to the small size of the pores. In some cases, other driving forces may become important, for example, osmotic forces in mixed solvents or in the presence of solutes. Capillary forces originate from the change in free surface energy, ΔE, when a solvent is spread on a ceramic surface

$$\Delta E = \gamma_{SL} + \gamma_{LV} - \gamma_{SV} \tag{25}$$

where γ_{SL}, γ_{LV}, and γ_{SV} are the specific energies of the solid–liquid, liquid–vapor, and solid–vapor interfaces, respectively. The force balance at the

three-phase line is described by Young's equation [34]

$$\gamma_{SV} = \gamma_{SL} + \gamma_{LV}\cos(\theta) \tag{26}$$

where θ is the contact angle. For $\theta > 90°$, the solvent does not spread on the solid surface, whereas spontaneous wetting and spreading occurs for $\theta = 0°$ where $\Delta E < 0$. The wetting of the pore walls by the solvent leads to a tensile stress in the liquid that can be described as a negative pressure. The pressure depends not only on the interfacial specific energies but also on the pore size. For a cylindrical capillary with radius, a, the capillary pressure, P_C, can be written as

$$P_C = -\frac{2(\gamma_{SV} - \gamma_{SL})}{a} = -\frac{2\gamma_{LV}\cos(\theta)}{a} \tag{27}$$

For a contact angle $\theta = 0°$, the curvature of the liquid–vapor interface equals the capillary radius. The pressure difference across the liquid–vapor interface of a cylindrical pore is $\Delta P = \gamma_{LV}/a$ as derived from the Laplace equation

$$\Delta P = \gamma_{LV}\left(\frac{1}{R_1} + \frac{1}{R_2}\right) \tag{28}$$

where R_1 and R_2 are the principal radii of the curved liquid–vapor interface.

Due to the capillary pressure, a tensile stress develops in the liquid, which is equivalent to a compressive force acting on the particle network of the green body. Thus, solvent is forced from the interior of the green body to the exterior surface as the particle network contracts. Accordingly, the volume change of the green body equals the solvent volume that has evaporated at the green body surface. The contraction of the particle network is characteristic for the first stage of the drying process. It is called constant rate period (CRP) because the green body weight decreases at a constant rate. The further the particle network is compressed, the stiffer it becomes. The end of the CRP is marked by a maximum in capillary pressure and, thus, cracking of the green body is most likely to occur at this point of the drying process. The stresses that may lead to cracking originate from local differences in capillary pressure and the corresponding differential shrinkage. Such differential strains are inevitable near the drying front where the local tension in the liquid is higher than in the saturated interior pore space. For example, during drying of a flat plate, the pressure raises in a parabolic fashion from the midplane towards the outer surfaces of the plate [39]. As is apparent from Eq. 27 [20, 40], the magnitude of the capillary pressure depends on the pore size. Therefore, drying stresses

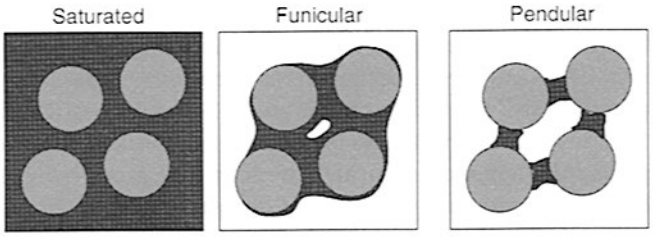

FIGURE 3.1.29 Schematic drawing of the solvent distribution in a porous body during different drying stages.

are more severe in gels with pore sizes in the nanometer range as compared to conventional ceramics with micron-sized particles. The magnitude of drying stresses is also expected to increase with the size of the green body and the drying rate [37].

At the end of the CRP, sometimes called leatherhard point or critical point, the network compressive strength exceeds the capillary pressure. Hence, further contraction is impossible and pores are partially drained, that is, the porous body is no longer saturated with solvent and enters a funicular state (Fig. 3.1.29). The term falling rate period (FRP) is used for this stage of the drying process because the rate of weight loss is decreased as compared to the CRP. During the FRP the drying front moves gradually into the interior of the green body.

Although the pores are becoming partially drained, the pore walls are still covered by a contiguous liquid film. The partial vapor pressure, p_V, of the solvent at the curved liquid–vapor interface is related to the tension, P, in the liquid or the interfacial energy, γ_{LV}, by

$$p_V = p_0 \exp\left(-\frac{PV_m}{R_g T}\right) = p_0 \exp\left(-\frac{2V_m \gamma_{LV} \cos\theta}{R_g T a}\right) \tag{29}$$

where p_0 is the equilibrium vapor pressure over a flat liquid–vapor interface, V_m the molar volume of the liquid, R_g the gas constant, and T the temperature. Evaporation takes place at the exterior green body surface when the ambient partial pressure is below p_V. The solvent is transported by liquid flow along the pressure gradient towards the exterior surface; transport via vapor diffusion through the drained pores is comparably small at this stage. The pressure driven flux of liquid through the porous body is described by an empirical expression known as Darcy's law

$$J = -\frac{D}{\eta}\nabla P \tag{30}$$

with D being the permeability of the porous structure and η the solvent viscosity. The lower the permeability, the higher is the resistance to liquid flow in the particle network and, thus, the greater is the pressure gradient needed to drain the porous body. The solvent evaporation at the surface is endothermal and leads to a lower temperature at the surface relative to both the ambient temperature and the temperature in the interior of the green body. This leads to a corresponding temperature dependent decrease in liquid surface tension and increase in vapor pressure at the surface, which further promotes the flow of liquid from the interior to the surface. The rate at which the drying front moves inside the porous body has been found to be inversely proportional to the square root of time [41].

The funicular state cannot be maintained any longer when the distance between the drying front and the green body surface is so large that the pressure gradient is insufficient to drive a liquid flow that balances the solvent evaporation at the surface. At this point a transition from the funicular to the pendular state (Fig. 3.1.29) takes place. In the pendular state, totally drained pores appear that are not connected by a liquid film to the liquid in the surrounding pores. Consequently, evaporation of solvent inside the porous network becomes large enough that diffusion of vapor through the empty pore space becomes the rate determining transport mechansim for solvent molecules. Fick's law links the diffusive flux, J_D, to the concentration gradient, ∇C, in the vapor phase

$$J_D = -D_C \nabla C \tag{31}$$

with D_C being the diffusion coefficient.

Willett *et al.* [42] have measured the capillary forces induced by pendular liquid bridges between sperical particles and showed that gravitational distortion and disjoining pressures have negligible effect on the measured attractive forces. Additionally, they developed a scaling method that could be used to establish closed-form expressions that accurately describe the measured force–distance curves.

It is apparent from the above discussion that both mass and heat transfer mechanisms are operative simultaneously during the drying process. The complex interplay of these processes determines the kinetics of the overall drying process. Moreover, the control of the drying conditions which affect the drying kinetics is not only decisive for the drying time but is also vital for any effort to minimize drying stresses and the risk of cracking and non-uniform deformation [36, 37]. The work of Ghosal *et al.* [43, 44] is one example that illustrates how modeling of the transport processes can be employed to predict and control appropriate drying conditions in industrial ceramic processing. These authors developed a one-dimensional physical model for the drying of gelcast ceramic

parts. By identifying the rate-limiting mechanisms for unidirectional solvent removal at all stages in the drying process they could apply comparably simple theoretical expressions to describe the drying process as a function of several controlled drying parameters, namely the partial solvent pressure, the drying temperature and the thickness of the gel-cast part.

3.1.5 GREEN BODY CHARACTERIZATION

In the past few years, the innovative use of new techniques for the characterization of ceramic green bodies allowed a significantly improved description of green body microstructures. Techniques like immersion microscopy and X-ray computed tomography have helped to gain a better understanding of microstructure evolution in the powder compaction process and they proved to aid in the identification of the origin and nature of strength-limiting defects. The main body of information available in the literature deals with the characterization of spray-dried granules and dry-pressed compacts, thus reflecting the dominating role of pressing techniques in the industrial manufacturing of ceramic parts.

3.1.5.1 MORPHOLOGY

Characteristic features of green body morphologies are typically in the 0.1–100 μm size range, which makes scanning electron microscopy (SEM) a versatile technique for morphology studies. The morphology of spray-dried granules and fracture surfaces of compacted green bodies are typical examples. Clearly, granule morphology is of importance in dry pressing operations since it will strongly influence particle packing during compaction and, thus, the size and number of pores in the green compact. SEM studies on granule shape and stereological evaluation of granule cross-sections have been used to investigate the correlation between suspension characteristics of a spray-dried slurry and the morphology of the resulting granules [45, 46]. It has been found that spray drying of flocculated, colloidally unstable powder suspensions will in general result in the formation of rather uniform and approximately spherical granules that do not contain big internal pores. In contrast, at identical spray-drying conditions irregularly shaped granules with large dimples or internal pores are formed when well dispersed, colloidally stable suspensions are spray dried. Additional results concerning the influence of spray-drying conditions suggest that the colloidal stability of spray-dried suspensions has a greater influence on the granule morphology than a moderate variation of spray drying parameters

such as inlet temperature of the drying chamber or flow rate of the feed slurry [47]. However, as discussed below, compacting and sintering different batches of spray-dried granules with practically identical morphology can still lead to considerable variations in sintered strength if they differ with respect to other granule properties (e.g. granule strength and binder distribution).

3.1.5.2 Mechanical Properties

Sufficient green body strength is required to prevent fracture or cracking during handling and drying. In some cases, the green strength may even be high enough to allow green machining, which is convenient for dimension control or the production of more complex shapes. In the case of dry pressing methods, however, the granule strength needs to be optimized in a way that both handling without granule fracture and substantial deformation or fracture during compaction is possible. In the past, mechanical characterization of green bodies has been limited almost exclusively to compression tests of single granules, granular beds, or dry green compacts. The compressive load required to crush a single granule, P_{max}, is determined in a diametral compression test and, assuming that the granule is spherical, can be related to the granule tensile strength, σ_T, by the equation

$$\sigma_T = \frac{2.8P_{max}}{\pi d^2} \tag{32}$$

where d is the granule diameter [44]. A similar equation can be derived for diametral compression testing of cylindrical powder compacts

$$\sigma_T = \frac{2P_{max}}{\pi dl} \tag{33}$$

where d is the sample diameter and l is the sample length.

Similar to the analysis of mechanical properties of sintered ceramic bodies, statistical analysis of experimentally obtained strength data represents a very useful and important approach for the evaluation of the influence of processing parameters and green body microstructure on the green strength [49]. The commonly used two-parameter Weibull model can be expressed as

$$\ln\ln\left(\frac{1}{1-P_F}\right) = m\ln\left(\frac{\sigma}{\sigma_0}\right) + C \tag{34}$$

with the probability P_F of specimen failure, the Weibull modulus m, the experimentally determined stress σ, a normalizing stress σ_0, and a constant factor C [50]. The slope of a linear fit to the strength data in a $\ln\ln(1/(1-P_F))$ ln versus σ plot delivers the Weibull modulus, which is often used as a measure of sample reliability. As discussed below in more detail, combining Weibull analysis and characterization of sample microstructure provides a powerful tool for identification of the nature and the formation mechanisms of fracture origins in ceramic green bodies.

Carnheim and Green [51] have recently evaluated several theoretical models for the description of elastic properties of granular compacts. If a number of simplifying assumptions are valid, all theoretical models can be represented by the same equation

$$\frac{E}{E_0} = \beta\phi^z \tag{35}$$

where ϕ is the particle packing fraction, β a constant prefactor, E the Young modulus of the compact, E_0 the Young modulus of a single particle, and z the density exponent [50]. The most important assumption included in this model is a constant a/D ratio, that is, the ratio of average particle diameter, D, and average diameter of the contact area between adjacent particles, a, is assumed to be independent of the applied compaction stress. Fitting Eq. 35 to experimental data gave density exponents much higher than predicted by the theoretical models, which led the authors to the conclusion that the a/D ratio varies with compression load [51]. Experimental data [51] and theoretical analysis [52] showed that such deviations from theoretical predictions occur in systems containing a compliant binder phase which can significantly influence the stiffness of a granular compact structure depending on the applied compaction stresses. Moreover, mechanical stresses in granular compacts are transmitted along force-chains [53] that comprise only a fraction of the total particle number and whose structure changes continuously in response to the increasing applied compaction stress. The theoretical models of the elastic compact behavior, however, are based on assumptions involving a static compact structure with all particles participating in the stress transfer.

Experimental compaction curves, that is, plots of overall sample density versus applied pressure, have been used frequently to describe the compaction behavior of granular beds in a die compaction process. A characteristic compaction curve is depicted schematically in Figure 3.1.30.

The compaction curve displays two distinctly different compaction stages; both show a linear $P-\rho$ relationship but with a much stronger P dependence of σ in stage II. The transition between stage I and II is sometimes referred to

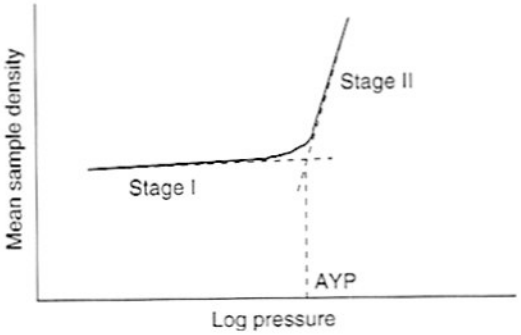

FIGURE 3.1.30 Typical compaction curve as observed in die compaction of granular powders.

as the apparent yield point (AYP) and can be estimated as the crossover point of the slopes of the two linear parts of the curve.

3.1.5.3 Microstructure

Information about the microstructure of a ceramic in the green state is of great value since inhomogeneities in the green body microstructure often persist in the sintering stage and are likely to become the origin of strength-limiting defects in the sintered body [16]. Many different types of microstructural defects may form in a ceramic processing scheme prior to sintering. In the case of advanced ceramics, pores are considered to be mainly responsible for the degradation of fracture strength. The green body microstructure is most often described in terms of overall sample density or density distributions. High green densities are advantageous for optimized densification at low sintering temperatures and a homogeneous density distribution minimizes the deteriorating effects of differential sintering. Additionally, a detailed description of defect populations present in the microstructure is desirable. This is related to the brittle nature of ceramic green bodies; their fracture mechanics are governed by parameters such as defect shape and defect size distribution rather than bulk densities [50].

Mercury intrusion porosimetry can be used to determine the volume fraction of interconnected internal pores in dry powder compacts and the corresponding green body bulk density. Assuming a cylindrical pore shape with radius r, the relationship between pore radius and external pressure can be described by the Young–Laplace equation

$$\Delta P = \frac{-2\gamma \cos\theta}{r} \tag{36}$$

where γ is the surface tension of the liquid and θ is the contact angle between the liquid and a pore wall.

For the investigation of highly compacted green bodies with a low pore number density and few interconnected pores immersion microscopy is preferred over mercury intrusion porosimetry. Immersion microscopy is an optical method for direct observation of green body microstructures [16]. Immersion of the specimen in a liquid with a refractive index equal to that of the powder particles eliminates reflection of light at the particle/liquid interface. The fraction of light, R, that is reflected at the interface depends on the matching of the refractive indices of the particle, n_1, and the immersion liquid, n_2, as expressed by the equation

$$R = \frac{\left((n_1/n_2) - 1\right)^2}{\left((n_1/n_2) + 1\right)^2} \tag{37}$$

The value of the relative refractive index $n' = n_1/n_2$ required for optimum performance depends on the features that are investigated. A value of $n' = 1$ is desirable when secondary phases, for example, binders, or particle orientation (by means of cross-polarized light) are in the focus of the investigation. A value of $n' = 1.02$–1.04 produces better optical contrast and is preferable for the detection of microstructural defects, such as pores and cracks [54].

Immersion microscopy has been used extensively to show the close relation between green body microstructure and mechanical strength of the sintered ceramic [Shinohara *et al.* 1995, 47, 55]. For example, correlating Weibull statistics of strength data with statistical data on pore size and number density of samples made at different process conditions illustrated with good accuracy that the relative differences in mean strength between samples where matched quantitatively by the relative difference in number density of the largest pores in these samples [47]. Clearly, this approach provides an excellent method to investigate the influence of processing parameters on the mechanical properties of green or sintered ceramic bodies. The immersion microscopy technique was further used to show the effect of granule properties on the microstructure of die-pressed granular compacts [45–47, 54–57]. Spray-dried granules under load may exhibit brittle fracture or plastic deformation depending on the granule density, binder content, binder distribution, and binder structure. In general, granules with a higher fracture strength are more likely to survive die pressing at high compaction stresses, which leads to an increased number of large, residual voids in the green compact that are not eliminated during sintering. In contrast, weak granules facilitate compression to high green densities, more uniform density distributions and smaller number densities of large pores. In principle, the influence of granule properties on the porosity in the

green compact vanishes at sufficiently high compaction stresses. In practice, however, uniaxial die-pressing at too high pressures results in internal cracks due to lamination [58] or requires a costly subsequent high-pressure CIP treatment [59]. The compaction behavior of spray-dried granules is also strongly influenced by the processing conditions during pressing. The relative humidity in particular affects the granule fracture strength and the intergranular and granule–die wall friction, all of which play an eminent role in the evolution of density profiles in the compact [56, 57, 60]. At low relative humidity, granules are more brittle which leads to lower overall densities but also to a more homogeneous density distribution. At high relative humidity the opposite trends are observed.

X-ray computed tomography has proven to be a powerful tool to determine internal density distributions of green bodies [60]. Density profiles can be generated with this technique by passing a finely collimated X-ray beam on a horizontal plane through the specimen while the material- and density-dependent X-ray transmission is recorded with a detector. In this process, the sample is continuously rotated and translates slowly past the detector in order to construct a two- or three-dimensional representation of the internal density distribution [61, 62]. Deis and Lannutti [60] used X-ray computed tomography to give a detailed picture of the evolution of localized high- and low-density regions during uniaxial die-pressing. They could also show that the stage I–II transition in the compaction curve (Fig. 3.1.35) is not attributed to two independent asynchronous densification mechanisms; particle rearrangement mechanisms and particle deformation (or fracture) mechanisms are both active at all compression stages but the relative importance of these two types of densification mechanisms varies substantially with respect to the spatial location in the die cavity [63]. During stage I, local high-density centers near the advancing ram grow until they finally join and form a layer of uniform density adjacent to the advancing ram, which marks the transition point between stage I and II. During stage II this high density layer expands toward the stationary ram in a wavelike manner. Based on these findings, the stage I–II transition was explained by a change in structural force transmission patterns. Compaction forces are transmitted at the granule–granule contact points, but during stage I, due to the irregular particle packing at low densities, a significant part of the applied pressure is directed toward the die wall and dissipated by intergranular friction. With increasing pressure, the density of the layer adjacent to the advancing ram increases and becomes more uniform due to deformation and fracture of granules. Accordingly, the intergranular contact area increases gradually and at the beginning of stage II the major part of the applied pressure is transmitted in the direction of the advancing ram, thus causing the much more efficient densification characteristic for stage II.

3.1.6 REMOVAL OF ORGANIC ADDITIVES

The risk of an uncontrolled release of large volumes of organic decomposition products at sintering temperatures makes it necessary to burn out the organic content at lower temperatures prior to sintering. The formation of excessive amounts of volatile decomposition products is unwanted because they create internal pressure gradients that lead to cracking, if they exceed the green body strength. Solvent extraction, that is, immersion of the green body in a fluid that dissolves the polymer, is an alternative method to remove the organic content, but suffers from problems with comparably high costs and environmental hazards [64].

With temperatures of about 300–700°C in the burn-out step, one can achieve slower decomposition kinetics and a better control of the debinding process, thus reducing the risk for crack formation in the green body. It is desirable to operate at temperatures where the partial pressure of volatiles formed by polymer decomposition is below 1 atm [36]. At higher temperatures, the local pressure is higher in the pores than at the external surface, which results in tensile stresses at the surface. Alternatively, it is possible to increase the ambient pressure to reduce the partial pressure of the volatiles [65].

In a ceramic green body, polymeric binders usually constitute the largest fraction of the organic phase compared to other organic components such as dispersants or plasticizers. There are several pathways for the decomposition of organic additives, depending on the chemical structure of the polymeric components, the burn-out temperature, and the composition of the solid and the gas phase. The reaction products that form in the decomposition process may be solid or volatile and the polymer degradation may be caused by thermal activation or by oxidative attack.

Analogous to green body drying, the pore size distribution in the green body has a large effect on the transport of reactants and reaction products. Similarly, the heat transfer is also affected by the pore dimensions, in addition to the influence of material dependent heat conductivities of the solid and the gas phase. Inappropriate heating conditions can lead to cracking induced by internal temperature gradients and the corresponding thermal stresses in the green body. Additional factors influencing the evolution of temperature gradients are endothermal or exothermal reactions involved in the polymer degradation process. As a consequence of the limited burn-out temperature relatively longer times are often needed to achieve complete removal of the organic green body content. In the case of forming techniques requiring a high binder content (e.g. extrusion and injection moulding) debinding times of up to several days may be necessary.

Polymer removal proceeds via chain scission induced by either thermal or oxidative degradation, followed by evaporation of the low-molecular-weight

fraction of the chain scission products [36]. Slow diffusive transport of oxygen through the pore space is often a rate determining process in oxidative polymer degradation. The kinetics of oxidative attack can be enhanced by the catalytic activity of metals, present in the ceramic body, for example, in form of metal oxides. Cyclization or cross-linking reactions on the other hand slow down polymer removal due to the resulting increase in polymer molecular weight. Most often it is required that polymeric additives depolymerize into volatile low-molecular-weight products rather than solid carbonaceous end-products that will remain in the green body after burn-out. In an oxidizing atmosphere, it is possible to remove residual carbon at temperatures below 800°C. In a reducing atmosphere, however, carbon will not be removed even at high sintering temperatures.

Lu and Lannutti [66] have investigated the effect of binder removal on the green body dimensional tolerances with X-ray computed tomography and *in situ* laser dilatometry. They showed that during debinding capillary force gradients cause the liquid binder to migrate to the high-density regions. This gives rise to a higher relative densification in the low-density regions. Therefore, green bodies with pronounced density gradients exhibit differential dimensional changes during binder burn-out. In contrast, samples with negligible density gradients showed uniform dimensional changes. It can be expected that the local redistribution of liquid binder is affected by the melt viscosity of the binder and the surface tension at the liquid–vapor interface. Based on these findings, it can be also be assumed that the total debinding time is determined by the binder removal from the high-density regions.

REFERENCES

1. Gotoh, K., and Higashitani, K., eds. (1997). *Powder Technology Handbook*. New York: Marcel Dekker, Inc.
2. Bergstrom, L. (1997). Hamaker constants of inorganic materials. *Advances in Colloid and Interface Science* 70: 125.
3. Roger H. French (2000). Origins and applications of London dispersion forces and Hamaker constants in ceramics. *J. Am. Ceram. Soc.* 83 (9): 2117–2146.
4. Rahaman, M. N., and NetLibrary Inc. (1995). *Ceramic Processing and Sintering*, New York: Marcel Dekker.
5. Hunter, R. J., and White, L. R. (1987). Foundations of colloid science. Oxford Oxfordshire New York: Clarendon Press; Oxford University Press.
6. Israelachvili, J. N. (1985). *Intermolecular and Surface Forces*. London: Academic Press.
7. Napper, D. H., and Hunter, R. J. (1972). Hydrosols in M.T.P. *Int. Rev. Sci. Phys. Chem. Ser. I.* 7: 241.
8. Smoluchowski Von, M. (1916). *Z. Phys.* 17: 557, 585.
9. Reed, J. S. (1995). *Principles of Ceramics Processing*, 2nd edn, New York: Wiley, pp. xxii, 658.

10. Krieger, I. M., and Dougherty, T. J. (1959). A mechanism for non-newtonian flow in suspensions of rigid spheres. *Transactions of the Society of Rheology* **3**: 137–152.
11. Krieger, I. M. (1972). Rheology of monodisperse lattices. *Advances in Colloid and Interface Science* **3**: 111–136.
12. Conley, J. R. F. (1996). Practical Dispersion: A Guide to Understanding and Formulating Slurries, New York: VCH, xviii, 446.
13. Dobiáa, B., Qiu, X., and Rybinski, W. V. (1999). Solid–liquid dispersions. *Surfactant Science Series*, Vol. 81, pp. vii, 562, New York: Marcel Dekker.
14. Cesarano, J., III, and Aksay, I. A. (1988). Processing of highly concentrated aqueous α-alumina suspensions stabilized with polyelectrolytes. *J. Am. Ceram. Soc.* **71**: 1062–1067.
15. Cesarano, J., Aksay, I. A., and Bleier, A. (1988). Stability of aqueous alpha-Al_2O_3 suspensions with poly (methacrylic acid) poly-electrolyte. *J. Am. Ceram Soc.* **71** (4): 250–255.
16. Sigmund, W. M., Bell, N. S., and Bergstrom, L. (2000). Novel powder-processing methods for advanced ceramics. *J. Am. Ceram. Soc.* **83**: 1557–1574.
17. Lange, F. F. (1989). Powder processing science and technology for increasing reliability. *J. Am. Ceram. Soc.* **72**: 3–15.
18. Horn, R. G. (1990). Surface forces and their action in ceramic materials. *J. Am. Ceram. Soc.* **73**: 1117–1135.
19. Lewis, J. A. (2000). Colloidal processing of ceramics. *J. Am. Ceram. Soc.* **83**: 2341–2359.
20. Myers, D. (1989). *Surfaces, Interfaces, and Colloids—Principles and Applications*, pp. 286–296. New York: VCH.
21. Baes, C. F., and Mesmer, R. (1986). *The Hydrolysis of Cations*. Malabar, Florida: Krieger Publishing Comp.
22. Roosen, A. (1988). *Ceram. Trans.* Vol. 1, Part B., Ceramic Powder Science, p. 675.
23. Böhnlein-Mauß, Sigmund, W., Wegner, W., Meyer, W. H., Heßel, F., Seitz, K., and Roosen, A. (1992). The function of polymers in the tape casting of alumina. *Adv. Mater.* **4**: 73–81.
24. Mistler, R. E., Runk, R., and Shanefield, D. (1978). Tapecasting of ceramics, *Ceramic Processing before Firing*, pp. 441–448, Onoda, G., and Hench, L., eds., New York: Wiley.
25. Paul, C. W., and Cotts, P. M. (1986). *Macromolecules* **19**: 692–699.
26. Napper, D. H. (1983). *Polymeric Stabilization of Colloidal Dispersions*. London: Academic Press, pp. xvi, 428.
27. Guo, J., and Lewis, J. A. (1999). Aggregation effects on compressive flow properties and drying behavior of colloidal silica suspensions. *J. Am. Ceram. Soc.* **82**: 2345–2358.
28. Mistler, R. E. (1998). Tape casting: past, present, future. *Am. Ceram. Soc. Bull.* **77**.
29. Shanefield, D. J. (1995). *Organic Additives and Ceramic Processing*, Boston, MA: Kluwer Academic.
30. Onoda, G. Y., Jr., and Hench, L. L. (1978). *Ceramic Processing before Firing*, New York: John Wiley and Sons.
31. Richerson, D. W. (1992). *Modern Ceramic Engineering*, New York: Marcel Dekker.
32. Greenwood, R., Kendall, K., and Bellon, O. (2001). A method for making alumina fibres by co-extrusion of an alumina and starch paste. *J. Eur. Ceram. Soc.* **21**: 507–513.
33. Von Hoy, C., Barda, A., Griffith, M., and Halloran, J. W. (1998). Microfabrication of ceramics by co-extrusion. *J. Am. Ceram. Soc.* **81**: 152–158.
34. Wright, J. F., Jr, and Reed, J. S. (2001). Polymer-plasticized ceramic extrusion. Part 1. *Am. Ceram. Soc. Bull.* **80**: 31–35.
35. Mutsuddy, B. C., and Ford, R. C. (1995). *Ceramic Injection Molding; Materials Technology Series*, London: Chapman & Hall.
36. Ring, T. A. (1996). *Fundamentals of Ceramic Powder Processing and Synthesis*, San Diego, CA: Academic Press.
37. Brinker, C. J., and Scherer, G. W. (1990). *Sol–Gel Science*, San Diego, CA: Academic Press.